AD-A167 025 PHASE COMPARISON TIME DELAY ESTIMATION USING WIDEBAND SIGNALS(U) PENNSYLVANIA STATE UNIV STATE COLLEGE APPLIED RESEARCH LAB J D HATLESTAD ET AL. APR 86 1/1

UNCLASSIFIED TR-86-03 F/G 17/2 NL

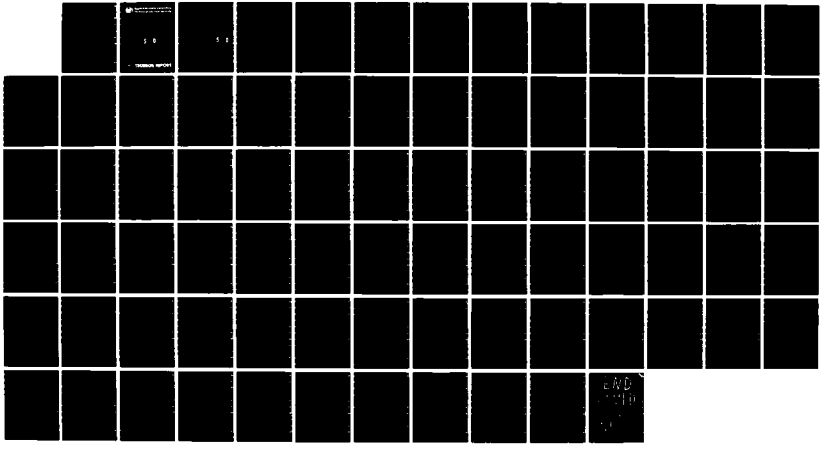

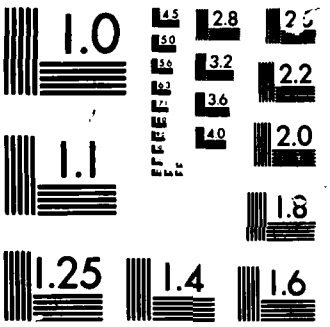

MICROCOPY CHART

Applied Research Laboratory
The Pennsylvania State University

(12)

PHASE COMPARISON TIME DELAY ESTIMATION USING WIDEBAND SIGNALS

by

J. D. Hatlestad and D. W. Ricker

ARL-TR-86-20

TECHNICAL REPORT

The Pennsylvania State University
Intercollege Research Programs and Facilities
APPLIED RESEARCH LABORATORY
P. O. Box 30
State College, PA 16804

12

PHASE COMPARISON TIME DELAY ESTIMATION USING WIDEBAND SIGNALS

by

J. D. Hatlestad and D. W. Ricker

Technical Report TR 86-03

April 1986

Supported by: Naval Sea Systems Command

L. R. Hettche, Director
Applied Research Laboratory

Unclassified
SECURITY CLASSIFICATION OF THIS PAGE

AD-A167025

REPORT DOCUMENTATION PAGE

1a. REPORT SECURITY CLASSIFICATION	1b. RESTRICTIVE MARKINGS
2a. SECURITY CLASSIFICATION AUTHORITY	3. DISTRIBUTION / AVAILABILITY OF REPORT Approved for public release; distribution unlimited.
2b. DECLASSIFICATION / DOWNGRADING SCHEDULE	
4 PERFORMING ORGANIZATION REPORT NUMBER(S)	5. MONITORING ORGANIZATION REPORT NUMBER(S)
6a NAME OF PERFORMING ORGANIZATION Applied Research Laboratory The Pennsylvania State Univ.	6b OFFICE SYMBOL (*If applicable*) ARL
6c ADDRESS (*City, State, and ZIP Code*) P. O. Box 30 State College, PA 16804	7a. NAME OF MONITORING ORGANIZATION 7b. ADDRESS (*City, State, and ZIP Code*)
8a. NAME OF FUNDING / SPONSORING ORGANIZATION Naval Sea Systems Command	8b. OFFICE SYMBOL (*If applicable*) NAVSEA
8c. ADDRESS (*City, State, and ZIP Code*) Department of the Navy Washington, DC 20362	9. PROCUREMENT INSTRUMENT IDENTIFICATION NUMBER 10. SOURCE OF FUNDING NUMBERS

PROGRAM ELEMENT NO.	PROJECT NO.	TASK NO.	WORK UNIT ACCESSION NO.

11 TITLE (*Include Security Classification*)
Phase Comparison Time Delay Estimation Using Wideband Signals

12 PERSONAL AUTHOR(S)
J. D. Hatlestad and D. W. Ricker

13a TYPE OF REPORT	13b. TIME COVERED FROM ____ TO ____	14. DATE OF REPORT (*Year, Month, Day*)	15. PAGE COUNT
M.S. Thesis		April 1986	76

16 SUPPLEMENTARY NOTATION

17 COSATI CODES		
FIELD	GROUP	SUB-GROUP

18. SUBJECT TERMS (*Continue on reverse if necessary and identify by block number*)
phase comparison time delay estimator; matched filters; large time-bandwidth; symmetric power spectra; white gaussian noise

19 ABSTRACT (*Continue on reverse if necessary and identify by block number*)

A method of phase comparison time delay estimation using large time-bandwidth product signals is presented. This method compares the phases of the matched filters for each channel, and it is shown that for signals with symmetric power spectra, a meaningful estimate of time delay can be expected from this phase information and knowledge of the carrier frequency of the signal.

The estimator is evaluated while operating in white Gaussian noise which is in general correlated between channels, and curves are given for the density function, mean, and variance of the estimator for various noise assumptions. The estimator is shown to take advantage of the processing gain of large time-bandwidth product signals to reduce the variance of the time delay estimate.

20 DISTRIBUTION / AVAILABILITY OF ABSTRACT	21. ABSTRACT SECURITY CLASSIFICATION	
☐ UNCLASSIFIED/UNLIMITED ☐ SAME AS RPT ☐ DTIC USERS		
22a NAME OF RESPONSIBLE INDIVIDUAL	22b TELEPHONE (*Include Area Code*)	22c. OFFICE SYMBOL

ABSTRACT

A method of phase comparison time delay estimation using large time-bandwidth product signals is presented. This method compares the phases of the matched filters for each channel, and it is shown that for signals with symmetric power spectra, a meaningful estimate of time delay can be extracted from this phase information and knowledge of the carrier frequency of the signal.

The estimator is evaluated while operating in white Gaussian noise which is in general correlated between channels, and curves are given for the density function, mean, and variance of the estimator for various noise assumptions. The estimator is shown to take advantage of the processing gain of large time-bandwidth product signals to reduce the variance of the time delay estimate.

TABLE OF CONTENTS

Page

ABSTRACT iii

LIST OF TABLES v

LIST OF FIGURES vi

ACKNOWLEDGEMENTS vii

CHAPTER

I. INTRODUCTION 1

II. RECEIVER STRUCTURE 3

III. UNCORRELATED NOISE 11

IV. CORRELATED NOISE 26

V. EFFECT OF τ-s MISMATCH 49

VI. SUMMARY AND CONCLUSIONS 60

APPENDIX A: CORRELATED NOISE MODEL 62

APPENDIX B: CHANGE IN CORRELATED PROPERTIES DUE TO COMPLEX MULTIPLICATION 64

APPENDIX C: FORTRAN SOURCE CODE FOR PHASE BIAS OF REAL-ENVELOPE SIGNALS 66

BIBLIOGRAPHY 68

LIST OF TABLES

Table		Page
3-1.	Theoretical Versus Sample Means and Variance	25
5-1.	Phase Bias for Real Envelope Signal	55

LIST OF FIGURES

Figure		Page
2-1	Receiver Structure	4
3-1	Probability Density of Estimator for Uncorrelated Noise, Nh=1,2,5,10.....	19
3-2	Probability Density of estimator for Uncorrelated Noise, Nh=10,20,50,100.....	20
3-3	Variance of Estimator for Uncorrelated Noise.....	21
3-4	Ambiguity Function for Signal Used in Example.....	24
4-1	Probability Density of Estimator, ρ=.67, λ=.67, ϕ_o=0.....	36
4-2	Mean Density of Estimator, ρ=.67, λ=.67, ϕ_o=0.....	37
4-3	Variance Density of Estimator, ρ=.67, λ=.67, ϕ_o=0.....	38
4-4	Probability Density of Estimator, ρ=0, λ=.9, ϕ_o=0.....	39
4-5	Mean Density of Estimator, ρ=0, λ=.9, ϕ_o=0.....	40
4-6	Variance Density of Estimator, ρ=0, λ=.9, ϕ_o=0.....	41
4-7	Probability Density of Estimator, ρ=.67, λ=.67, ϕ_o=0.....	42
4-8	Mean Density of Estimator, ρ=.67, λ=.67, ϕ_o=0.....	43
4-9	Variance Density of Estimator, ρ=.67, λ=.67, ϕ_o=0.....	44
4-10	Probability Density of Estimator, ρ=.9, λ=0,ϕ_o=0.....	45
4-11	Mean Density of Estimator, ρ=.9, λ=0,ϕ_o=0.....	46
4-12	Variance Density of Estimator, ρ=.9, λ=0,ϕ_o=0.....	47

ACKNOWLEDGEMENTS

I would like to thank my committee members for their helpful criticisms and suggestions regarding this work. In particular, I would like to thank Dr. Dennis W. Ricker for originally suggesting my thesis topic, and for providing continued support throughout the research and writing periods. I would also like to thank Michael Matuson and John Sacha for their help in working out some of the details, and David Drumheller for his help in designing the signal used in the examples.

Additionally, I would like to thank Phyllis McGarvey for her work in typing this thesis.

This work was supported by the Applied Research Laboratory of The Pennsylvania State University under contract with Naval Sea Systems Command.

CHAPTER 1

INTRODUCTION

The problem of time delay estimation has received much attention in the literature[1-6]. In its simplest terms, the problem is to estimate the time difference of arrival of similar signals in two different channels. In general, the literature can be divided into two distinct categories passive and echo location.

In the passive mode, the receiver "listens" to a source in each of two receiver channels, and estimates the time difference between the two channels. In this case, very little may be known about the form of the signal. In echo location, a signal is transmitted in the channels, and the receiver "listens" for reflections in the channel. Here the signal form is known to be a (possibly distorted) time delayed replica of the transmitted signal, and the task is to measure the difference of the time delays in the channels.

In each of these modes of operation there are two common methods used to estimate the time delay: cross-correlation methods, and phase comparison methods. The first of these methods performs a cross-correlation of the two received signals, selecting as the estimate of the time delay that value which maximizes the magnitude of the cross-correlation.

In the phase comparison method, the analytic signal from one channel is conjugated and multiplied by the signal from the other channel and the phase of the resultant product is averaged over the time

duration of the signal. In order to assign a meaningful estimate of the time delay from the phase information, the signal must be assumed narrowband.

In the literature cited above, these estimators and variants thereof have been extensively analyzed under various hypotheses.

This thesis presents a method of time delay estimation which was originally developed by Ricker[7]. This method is inherently an echo location estimator of time delay which uses a comparison of the phase of the matched filter for each channel to estimate the delay. It will be seen that, under the proper assumptions, this estimator is capable of using large time-bandwidth product signals and still giving a meaningful estimate of the time delay from the phase information.

Other advantages of this method include the fact that it handles Doppler-shifted channels with ease, and that with proper signal design, it can isolate multiple scatterers in the channels and estimate the time difference for each scatterer. With this estimator, one may utilize signals with large time-bandwidth products that resolve well both in time and in frequency so that one can simultaneously estimate the total propagation delay, the time stretch (Doppler), and the time difference of arrival.

The next chapter will present the receiver structure and the estimation procedure. Chapters 3, 4 and 5 will evaluate the performance of the receiver operating in additive white Gaussian noise, and Chapter 6 will summarize and suggest further work in this area.

CHAPTER 2

RECEIVER STRUCTURE

This chapter will discuss the method in which the received signals are processed, and will present notation and assumptions that will be used in the chapters that follow. The receiver structure is shown in Figure 2-1. It is assumed that a signal $f(t)e^{j\omega_o t}$, was transmitted and that the received signals, $r_1(t_i)$ and $r_2(t_i)$, are samples of two time-delayed, time-stretched replicas of the transmitted signal plus additive noise. The function $f(t)$ is known as the complex envelope of the signal, and ω_o is equal to $2\pi f_o$, where f_o is the carrier frequency. The received signals, r_1 and r_2 can be written as follows

$$r_1(t_i) = \sqrt{E_o}\, f[s(t_i-\tau_1)]e^{j\omega_o s(t_i-\tau_1)} + n_1(t_i)$$

$$r_2(t_i) = \sqrt{E_o}\, f[s(t_i-\tau_2)]e^{j\omega_o s(t_i-\tau_2)} + n_2(t_i)$$

It is assumed both signals are of the same energy, and that the complex envelope is normalized such that

$$\sum_{i=1}^{N} \left| f[s(t_i-\tau_k)] \right|^2 = 1 \qquad k = 1,2 \qquad (2\text{-}1)$$

so that in the absence of noise, the energy of each sampled signal is E_o. The time-stretch factor, s, is assumed to be the same in each channel, and is related to the Doppler shift, ϕ_d, as

$$\phi_d = \left(\frac{s-1}{s}\right) f_o \; . \qquad (2\text{-}2)$$

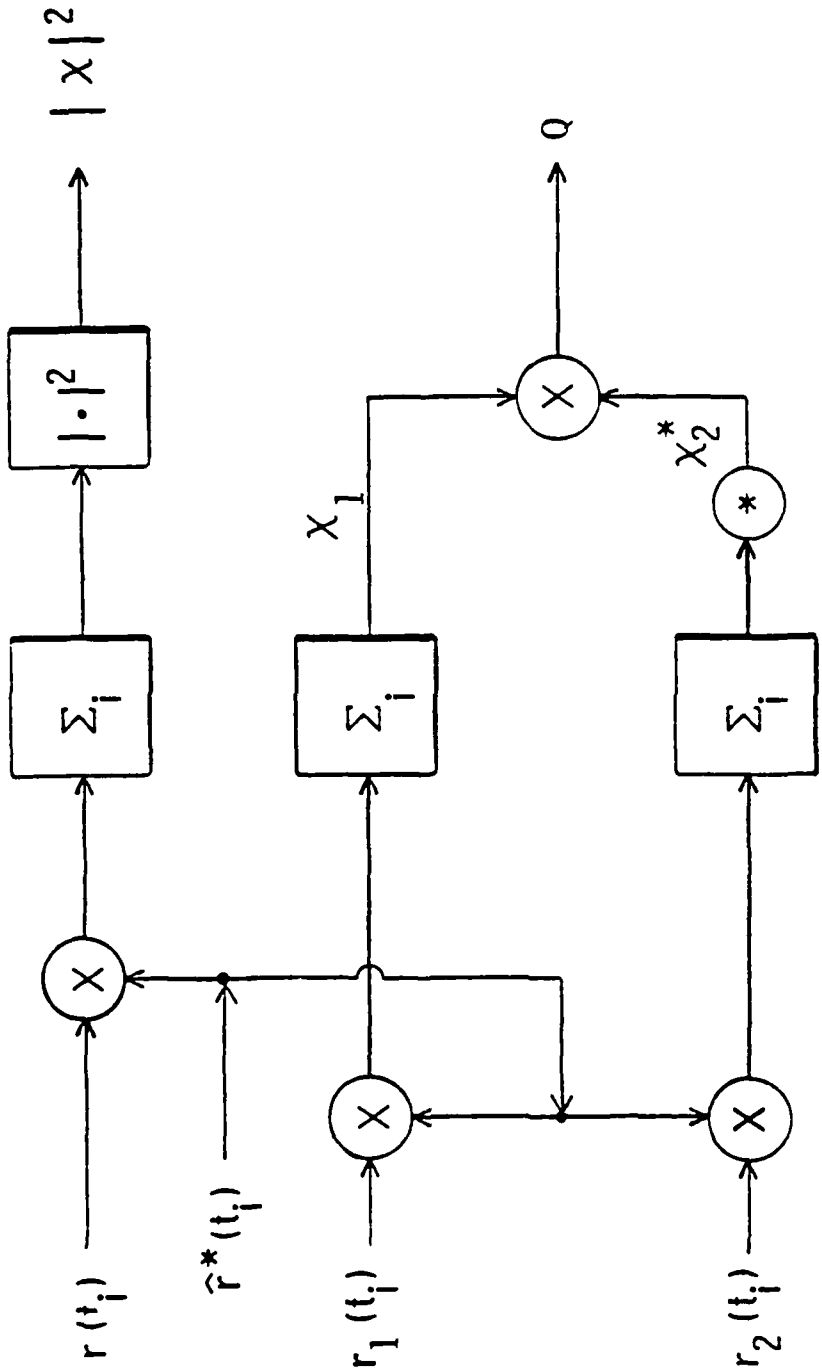

Figure 2-1: Receiver Structure

The time delays for each channel are denoted by τ_1 and τ_2, and the difference in time delays, $\Delta\tau = \tau_2 - \tau_1$, is the quantity to be estimated.

The noises $n_1(t_i)$ and $n_2(t_i)$ are assumed to be white, complex processes with circular symmetry[8,9], and with variance of real and imaginary parts equal to σ_n^2. The real and imaginary components for each channel are denoted as

$$n_k(t_i) = x_k(t_i) + jy_k(t_i) \qquad k = 1,2.$$

The received signals are processed according to Figure 2-1. The processing signal, $\hat{r}(t_i)$, is a time-delayed, time-stretched replica of the transmitted signal with hypothesis time-delay and time-stretch values of $\hat{\tau}$ and $\hat{s}$ obtained through some previous estimation procedure. The processing signal is denoted as follows:

$$\hat{r}(t_i) = f^*[\hat{s}(t_i-\hat{\tau})]e^{-j\omega_o\hat{s}(t_i-\hat{\tau})} .$$

The processing signal is assumed normalized to unit energy, i.e.

$$\sum_{i=1}^{N} \left| \hat{r}(t_i) \right|^2 = \sum_{i=1}^{N} \left| f[\hat{s}(t_i-\hat{\tau})] \right|^2 = 1.$$

In the absence of noise, the output of each summation in Figure 2-1 is

$$x_k = \sum_{i=1}^{N} \hat{r}(t_i) r_k(t_i)$$

$$= \sqrt{E_o} \sum_{i=1}^{N} f^*[\hat{s}(t_i-\hat{\tau})] f[s(t_i-\tau_k)] e^{j\omega_o[s(t_i-\tau_k)-\hat{s}(t_i-\hat{\tau})]} \qquad (2\text{-}3)$$

which, when viewed as a function of $\hat{\tau}$ and $\hat{s}$, can be considered as a two-dimensional correlation between the received and processing signals.

The estimates, $\hat{\tau}$ and $\hat{s}$, are often obtained by processing the received signal with a matched filter. The matched filter concept is based on the examination of the magnitude-squared of a function $\chi(\tau,s,\hat{\tau},\hat{s})$ over an appropriate grid of $\hat{\tau}$ and $\hat{s}$ values, choosing as the estimate of the time-delay and time-stretch those $\hat{\tau},\hat{s}$ pairs which maximize the magnitude squared, $|\chi(\tau,s,\hat{\tau},\hat{s})|^2$. Note that for signals with sufficient resolution, the matched filter approach is capable of resolving multiple reflections, identifying the τ and s values of each reflector as distinct maxima on the $\hat{\tau},\hat{s}$ grid.

An important function that arises out of the discussion of matched-filters is the ambiguity function. The ambiguity function depends only on the particular signal employed, and is equivalent to the matched filter for a noiseless scattering channel consisting of a point scatterer. The accuracy with which one can estimate time-delay and -stretch depends on the behavior of the signal ambiguity function near the origin. For the reader unfamiliar with matched filter concepts, rather thorough treatments are given in Van Trees[10], and in Cook and Bernfeld[11] for the narrowband case, and in papers by Altes[12,13] for the wideband formulation.

The time delay estimator of Figure 2-1 works as follows. First, the received signal, $r(t)$, representing a composite of the signals $r_1(t)$ and $r_2(t)$ (or a related signal) is matched-filtered over an appropriate $\hat{\tau}$-$\hat{s}$ grid, yielding $|\chi(\tau,s,\hat{\tau},\hat{s})|^2$. This function is examined over

the grid, with those peaks that are above a pre-selected threshold representing substantial reflections in the channel with different time-delay and -stretch values estimated by the corresponding $\hat{\tau}$ and $\hat{s}$ values.

Once a peak has been located, the $\hat{\tau}$ and $\hat{s}$ values corresponding to the peak are used to process the received signal for channels 1 and 2, yielding $\chi_1(\tau_1,s,\hat{\tau},\hat{s})$ and $\chi_2(\tau_2,s,\hat{\tau},\hat{s})$. For each peak, the complex numbers $\chi_1(\tau_1,s,\hat{\tau},\hat{s})$ and $\chi_2^*(\tau_2,s,\hat{\tau},\hat{s})$ are multiplied together, yielding (in the absence of noise)

$$Q = \chi_1\chi_2^* = E_o\cdot\Big(\sum_i f^*[\hat{s}(t_i-\hat{\tau})]f[s(t_i-\tau_1)]e^{j\omega_o(s-\hat{s})t_i}\Big)\cdot$$

$$\Big(\sum_i f[\hat{s}(t_i-\hat{\tau})]f^*[s(t_i-\tau_2)]e^{-j\omega_o(s-\hat{s})t_i}\Big)e^{j\omega_o s(\tau_2-\tau_1)}$$

$$= E_o\cdot\Big(\sum_{ij} f^*[\hat{s}(t_i-\hat{\tau})]f[s(t_i-\tau_1)]$$

$$f[\hat{s}(t_j-\hat{\tau})]f^*[s(t_j-\tau_2)]e^{j\omega_o(s-\hat{s})(t_i-t_j)}\Big)e^{j\omega_o s(\tau_2-\tau_1)} \qquad (2\text{-}4)$$

If the time-stretch estimate is assumed correct (i.e $\hat{s}$=s), the first line of (2-4) reduces to

$$Q = E_o\cdot\Big(\sum_i f^*[\hat{s}(t_i-\hat{\tau})]f[\hat{s}(t_i-\tau_1)]\Big)\cdot$$

$$\Big(\sum_i f[\hat{s}(t_i-\hat{\tau})]f^*[\hat{s}(t_i-\tau_2)]\Big)e^{j\omega_o\hat{s}(\tau_2-\tau_1)}$$

$$= E_o\cdot(A_1A_2^*)e^{j\phi_o} \qquad (2\text{-}5)$$

where

$$A_k = \sum_i f^*[s(t_i-\hat{\tau})]f[s(t_i-\tau_k)],$$

$$\phi_o = \omega_o s(\tau_2-\tau_1).$$

Hence, it is seen that if the time-stretch estimate is correct, the time difference of arrival can be obtained from the phase of Q as

$$\Delta\hat{\tau} = \frac{\phi_o}{\omega_o s}$$

if the quantity $(A_1 A_2^*)$ is real. Note that if $\tau_2 = \tau_1$, then $A_2 = A_1$ so that the quantity $A_1 A_2^*$ is real. However, with arbitrary $\Delta\tau$, A_1 and A_2 must be real independent of one another for most signals of interest, and it is desired to find sufficent conditions for which this occurs. To do this it is more convenient to utilize the continuous-time domain. In this domain

$$A_k = \int f^*(st-s\hat{\tau})f(st-s\tau_k)dt,$$

where the energy conserving factors have been ignored, as they are unimportant in the discussion. Defining

$$g(u) = f(u-a) \quad <=> \quad G(\omega) = e^{-j\omega a}F(\omega)$$

$$h(u) = f(u-b) \quad <=> \quad H(\omega) = e^{-j\omega b}F(\omega),$$

Parseval's relation,

$$\int_{-\infty}^{\infty} g^*(u)h(u)du = \int_{-\infty}^{\infty} G^*(\omega)H(\omega)d\omega$$

can be used to obtain

$$A_k = \int_{-\infty}^{\infty} G^*(\omega)H(\omega)d\omega = \int_{-\infty}^{\infty} |F(\omega)|^2 \, e^{j\omega s(\tau_k - \hat{\tau})} d\omega.$$

If $|F(-\omega)| = |F(\omega)|$, this reduces to

$$A_k = 2 \int_{o}^{\infty} |F(\omega)|^2 \cos \omega s(\tau_k - \hat{\tau}) d\omega, \qquad (2\text{-}6)$$

which is a real quantity. Hence, a sufficient condition for A_k to be real has been established. If the complex envelope has a symmetric power spectrum, $|F(-\omega)|^2 = |F(\omega)|^2$, then A_k is real. Note that this is dependent on the proper time-stretch estimate but is independent of the delay estimate. Throughout this thesis, it is assumed that this condition is satisfied so that A_1 and A_2 will be real quantities.

The performance of this estimator depends on two factors. First, the additive noise inherent in the channels will degrade performance by adding unwanted terms to (2-5), thereby corrupting the phase, ϕ_o. Second, the estimates, $\hat{\tau}$ and $\hat{s}$ will not exactly match the true values. If the estimate $\hat{\tau}$ is reasonably close to the true values τ_1 and τ_2, performance will not be adversely affected, since the only effect of this is that the factors A_1 and A_2 in (2-5) will become smaller relative to the additive noise terms as can be seen from the cosine term in (2-6). If the estimate $\hat{s}$ is incorrect, however, the estimator becomes biased due to the additional exponential that appears in (2-4). The τ and s estimates obtained from the matched filter will obviously become less accurate as the noise level increases.

In Chapters 3 and 4, the first of these problems is addressed, i.e. that of the unwanted noise terms. In these chapters it is assumed that the estimates of τ and s are correct. In Chapter 5, the effect of a τ-s mismatch is discussed using a Cramér-Rao lower bound approach. To simplify the analysis and notation, it is assumed throughout the following that the channels contain only one scatterer.

CHAPTER 3

UNCORRELATED NOISE

The first case to be considered is that of the receiver operating in white Gaussian noise uncorrelated between channels. The complex noise process is assumed stationary, ergodic, zero mean, circularly symmetric, with variance of real and imaginary parts equal to σ_n^2. The real and imaginary components for each channel are independent, and are denoted as follows:

$$n_1(t_i) = x_1(t_i) + jy_1(t_i)$$

$$n_2(t_i) = x_2(t_i) + jy_2(t_i)$$

or more succinctly as

$$n_{ki} = x_{ki} + jy_{ki} \qquad k = 1,2$$

where the first subscript identifies the channel, and the second is the time index.

The white noise assumption requires that

$$E\{x_{ki}\ x_{kj}\} = E\{y_{ki}\ y_{kj}\} = \sigma_n^2\ \delta_{ij} \qquad k = 1,2$$

where δ_{ij} is the Kronecker delta

$$\delta_{ij} = \begin{matrix} 1, i=j \\ 0, i\neq j \end{matrix} .$$

Circular symmetry requires that

$$E\{x_{ki}\ y_{ki}\} = 0 \text{ for all } i;\ k = 1,2$$

and the additional assumption of noise uncorrelated between channels requires that

$$E\{x_{1i}x_{2j}\} = E\{y_{1i}\ y_{2j}\} = E\{x_{1i}\ y_{2j}\} = E\{x_{2i}\ y_{1j}\} = 0$$

$$\text{for all } i,j. \qquad (3\text{-}1)$$

The magnitude-squared of the noise process has expectation

$$E\{|n_{ki}|^2\} = E\{x_{ki}^2 + y_{ki}^2\} = 2\sigma_n^2 \qquad k = 1,2.$$

The received signal for each channel at time t_i is

$$r_k(t_i) = \sqrt{E_o}\, f[s(t_i-\tau_k)]e^{j\omega_o s(t_i-\tau_k)} + n_k(t_i)$$

or

$$r_{ki} = \sqrt{E_o}\, f_{ki}\, e^{j\omega_o s(t_i-\tau_k)} + n_{ki}$$

where $f_{ki} \equiv f[s(t_i-\tau_k)]$ is the complex envelope of the received signal. If the processing signal $\hat{r}(t_i)$ is denoted as follows:

$$\hat{r}(t_i) = \hat{r}_i = \hat{f}_i\, e^{-j\omega_o \hat{s}(t_i-\hat{\tau})}$$

where $\hat{f}_i \equiv f^*[\hat{s}(t_i-\hat{\tau})]$ represents the complex envelope of the processing signal, then the output of each summation block in Figure 2-1 can be written

$$\chi_k = \sum_i \hat{r}_i\, r_{ki} = \sum_i \hat{f}_i\, e^{-j\omega_o \hat{s}(t_i-\hat{\tau})} \left[\sqrt{E_o}\, f_{ki} e^{j\omega_o s(t_i-\tau_k)} + n_{ki}\right]$$

$$= \sum_i \left[\sqrt{E_o}\, \hat{f}_i f_{ki}\, e^{j\omega_o[(s-\hat{s})t_i + \hat{s}\hat{\tau} - s\tau_k]} + n_{ki}\hat{f}_i e^{-j\omega_o \hat{s}(t_i-\hat{\tau})}\right]$$

$$= \sum_i \left[\sqrt{E_o}\, \hat{f}_i f_{ki}\, e^{j\omega_o \hat{s}(\hat{\tau}-\tau_k)} + n_{ki}\hat{f}_i e^{-j\omega_o \hat{s}(t_i-\hat{\tau})}\right] \quad (\text{if } \hat{s}=s) \qquad (3\text{-}2)$$

where the last line assumes the proper time-stretch estimate, $\hat{s} = s$.

Since the Gaussian noise components are all assumed independent of one another, the explicit and implicit phase factors in the second term of (3-2) can be absorbed into the noise process without altering the statistics of the situation. This yields

$$\chi_k = \sqrt{E_o}\, e^{j\omega_o \hat{s}(\hat{\tau}-\tau_k)} \cdot \sum_i \hat{f}_i f_{ki} + \sum_i |\hat{f}_i| n_{ki} \qquad k = 1,2. \quad (3\text{-}3)$$

The second term, being the sum of independent, zero-mean Gaussians is itself a zero-mean Gaussian, which shall be denoted by η_k. The real and imaginary parts of this term have variance

$$\sigma_\eta^2 = \sigma_n^2 \sum_i |\hat{f}_i|^2 = \sigma_n^2 ,$$

since $\Sigma\ |\hat{f}_i|^2 = 1$, so that (3-3) can be written as

$$\chi_k = \sqrt{E_o}\, A_k\, e^{j\omega_o \hat{s}(\hat{\tau}-\tau_k)} + \eta_k \qquad k = 1,2,$$

where $A_k = \Sigma\ \hat{f}_i f_{ki}$.

The output, Q, of the estimator of Figure 2-1 is then

$$Q = \chi_1 \chi_2^* = \left|\sqrt{E_o}\, A_1 e^{j\omega_o \hat{s}(\hat{\tau}-\tau_1)} + \eta_1\right| \cdot \left|\sqrt{E_o}\, A_2 e^{-j\omega_o \hat{s}(\hat{\tau}-\tau_2)} + \eta_2^*\right|$$

$$= E_o A_1 A_2\, e^{j\omega_o \hat{s}(\tau_2-\tau_1)} + \sqrt{E_o}\, A_2 \eta_1 + \sqrt{E_o}\, A_1 \eta_2^* + \eta_1 \eta_2^* \qquad (3\text{-}4)$$

where, as above, the complex exponentials have been absorbed into the noise terms without altering the statistics.

It has been previously assumed that $\hat{s}$=s. If it is now also assumed that the time difference of arrival, $\Delta\tau$, is small and that the time delay estimate, $\hat{\tau}$ is accurate such that $\hat{\tau} = \tau_k$ (k = 1,2), then $f_{ki} = \hat{f}_i$, so that $A_k = \Sigma\ |\hat{f}_i|^2 = 1$.

To see what is meant by the words "small" and "accurate," one needs to examine (2-6) where it is seen that if $\cos \omega_{max}\hat{s}(\tau_k-\hat{\tau}) \approx 1$, then A_k will be at its maximum, which is 1. Here ω_{max} denotes the maximum frequency of the complex envelope (i.e., ω_{max} equals one-half the signal bandwidth). In this case (3-4) reduces to

$$Q = E_o e^{j\omega_o \hat{s}(\tau_2-\tau_1)} + \sqrt{E_o}\, n_1 + \sqrt{E_o}\, n_2^* + n_1 n_2^* \qquad (3\text{-}5)$$

The presence of the last term in (3-5) renders further analysis intractable, so it is desired to quantify conditions under which this term becomes negligible. The expectation of the magnitude-squared of of the process can be found as

$$\begin{aligned} E\{|n_1 n_2^*|^2\} &= E\{[\mathrm{Re}(n_1 n_2^*)]^2\} + E\{[\mathrm{Im}(n_1 n_2^*)]^2\} \\ &= 4\sigma_n^4 , \end{aligned}$$

where $E\{\cdot\}$ is the expectation operator. Thus, if the input signal-to-noise ratio is defined as

$$h = \frac{\text{Input Signal Energy}}{\text{Expected Input Noise Energy}} = \frac{E_o}{N \cdot E\{|n_{ki}|^2\}} = \frac{E_o}{2N\sigma_n^2} ,$$

then the ratio of the magnitude-squared of the first term of (3-5) to that of the second or third term has expectation

$$\frac{E_o^2}{E\{E_o \cdot |n_k|^2\}} = \frac{E_o}{2\sigma_n^2} = Nh \qquad (3\text{-}6)$$

while the ratio of the magnitude of the first term to that of the last term has expectation

$$\frac{E_o^2}{4\sigma_n^4} = (Nh)^2 \ . \qquad (3\text{-}7)$$

Here, as in the previous chapter, N is the number of input samples. By comparing (3-6) and (3-7), it is seen that the last term of (3-5) is of second order. For example, if there is a 0dB input SNR (h=1) and there are 1000 input samples, then the second and third terms are 30dB below the first, while the last term is 60dB below the first. For the rest of the development, it is assumed that the quantity Nh is large enough so that the last term of (3-5) can be ignored. It will be seen that for values of Nh as small as 10, this approximation yields variances consistent with those obtained through computer simulations.

It is seen that for large Nh, the output SNR, given approximately by (3-6), is N times as large as the input SNR. The factor N can thus be considered as a processing gain. For a receiver sampling at a frequency equal to the bandwidth of the signal, N is equal to the time-bandwidth product of the signal, so that the receiver structure of Figure 2-1 is seen to have a processing gain equal to the time-bandwidth product of the signal.

Defining η_3 such that

$$\eta_3 = \sqrt{E_o}\ (\eta_1+\eta_2^*),$$

(3-5) reduces to

$$Q = E_o e^{j\omega_o \hat{s}(\tau_2-\tau_1)} + \eta_3, \qquad (3\text{-}8)$$

where η_3 is a complex Gaussian process with variance of real and imaginary parts equal to

$$\sigma_3^2 = 2E_o\sigma_n^2 \ . \qquad (3\text{-}9)$$

Q can be written in terms of its real and imaginary parts as

$$\begin{aligned} Q &= E_o e^{j\phi_o} + \eta_3 \\ &= E_o(\cos\phi_o + j\sin\phi_o) + u+jv \\ &= a + u + j(b+v) \end{aligned}$$

where

$$\phi_o = \omega_o \hat{s}(\tau_2-\tau_1)$$

$$a = E_o\cos\phi_o,\ b = E_o\sin\phi_o$$

$$u = \mathrm{Re}\{\eta_3\},\ \mathrm{var}(u) = \sigma_3^2$$

$$v = \mathrm{Im}\{\eta_3\},\ \mathrm{var}(v) = \sigma_3^2\ ,$$

so that our estimate of ϕ_o, denoted by ϕ, is

$$\phi = \tan^{-1}\left(\frac{b+v}{a+u}\right). \qquad (3\text{-}10)$$

In the absence of noise it is noticed that $\phi \to \phi_o$ as desired.

In order to evaluate the performance of this estimator, it is desired to find the probability density function for ϕ, denoted by $f(\phi)$. The density function, $f(\phi)$ would be more precisely notated as $f(\phi|\phi_o)$, and might be more properly regarded as a likelihood function.[14] Also, it is noted that the estimator to be derived is a maximum likelihood estimator[11,15] of ϕ_o for the uncorrelated noise case.

The numerator and denominator of the arctan argument in (3-10) are independent and have Gaussian densities with mean b and a, respectively. The joint density for numerator and denominator is thus the product of the two marginal Gaussian densities, and to find the density for ϕ, one may convert to polar coordinates as follows, and integrate over $0 < r < \infty$. Letting $u+a = r\cos\phi$ and $v+b = r\sin\phi$, the joint density becomes

$$f(u,v) = \frac{1}{2\pi\sigma_3^2} \exp \frac{-1}{2\sigma_3^2} (u^2+v^2) \quad \rightarrow$$

$$f(r,\phi) = \frac{1}{2\pi\sigma_3^2} r \exp \frac{-1}{2\sigma_3^2} [(r\cos\phi-a)^2 + (r\sin\phi-b)^2] ,$$

where the factor r is the Jacobian of the transformation. The desired density is obtained by integrating over r:

$$f(\phi) = \int_o^\infty f(r,\phi)dr$$

$$= \frac{1}{2\pi\sigma_3^2} \exp \frac{-1}{2\sigma_3^2} [a^2+b^2] \cdot \int_o^\infty r \exp \frac{-1}{2\sigma_3^2} [r^2 - 2r(a\cos\phi + b\sin\phi)]dr.$$

Recalling that $a = E_o\cos\phi_o$ and $b = E_o\sin\phi_o$, and using a well known trigonometric identify, the above expression becomes

$$f(\phi) = \frac{1}{2\pi\sigma_3^2} \exp \frac{-E_o^2}{2\sigma_3^2} \cdot \int_o^\infty r \exp \frac{-1}{2\sigma_3^2} [r^2 - 2E_o r\cos(\phi-\phi_o)]dr,$$

or, making a change of integration variable,

$$f(\phi) = \frac{E_o^2}{2\pi\sigma_3^2} \int_o^\infty r \exp \frac{-E_o^2}{2\sigma_3^2} [r^2 - 2\cos(\phi-\phi_o)r + 1]dr,$$

which is a function only of $\phi-\phi_o$ and $(\frac{E_o}{\sigma_3})^2$. Recall that $\sigma_3^2 = 2E_o\sigma_n^2$, and $h = E_o/2N\sigma_n^2$, so that

$$\frac{E_o^2}{\sigma_3^2} = \frac{E_o^2}{2E_o^2\sigma_n} = Nh.$$

Here again, h is the input signal to noise ratio, and N is the number of input samples. Finally, then, the density is written

$$f(\phi) = \frac{Nh}{2\pi} e^{\frac{-Nh}{2}} \int_0^{\infty} r \exp \frac{-Nh}{2} [r^2 - 2 \cos(\phi-\phi_o)r]dr, \qquad (3\text{-}11)$$

which is a function only of $\phi-\phi_o$ and the quantity Nh.

Unfortunately, the density given by (3-11) cannot be expressed in closed form. The integral in (3-11) can be found in the tables by Gradshteyn and Ryzhik[16] (#3.462.5), where it is expressed in terms of the error function, but the solution is only valid in our case for $\cos(\phi-\phi_o) < 0$. The density of (3-11) is integrated numerically on a VAX 11/782, yielding the curves in Figures 3-1 and 3-2. Note that although these densities are defined over $-\pi < \phi-\phi_o < \pi$, in Figures 3-1 and 3-2 they are shown over a smaller range to better see their shape. Also, a curve of the variance as a function of the output signal to noise ratio Nh was generated digitally, yielding Figure 3-3.

It must be noted that the moment quantities depend on the integration limits chosen. Mathematically, any limits of the form $\theta < \phi < \theta + 2\pi$ will do, however for the application here, the choice is clear. Choosing the limits $\phi_o-\pi < \phi < \phi_o+\pi$, the mean, μ, is given by

$$\mu = \int_{\phi_o-\pi}^{\phi_o+\pi} \phi f(\phi)d\phi = \int_{-\pi}^{\pi} (\phi+\phi_o)f(\phi+\phi_o)d\phi$$

$$= \int_{-\pi}^{\pi} \phi f(\phi+\phi_o)d\phi + \phi_o \int_{-\pi}^{\pi} f(\phi+\phi_o)d\phi$$

$$= 0 + \phi_o = \phi_o,$$

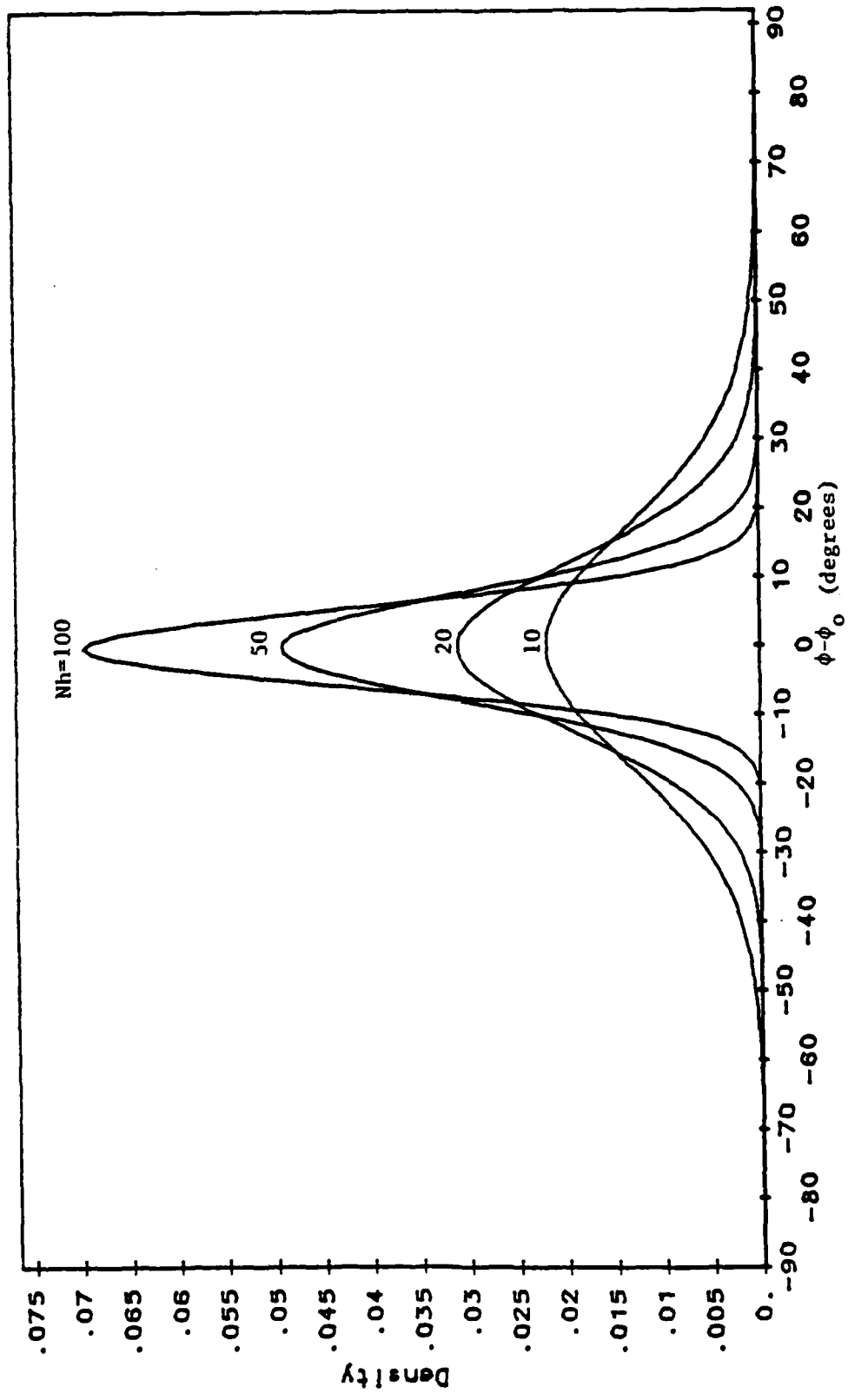

Figure 3-1: Probability Density of Estimator for Uncorrelated Noise; Nh=10,20,50,100

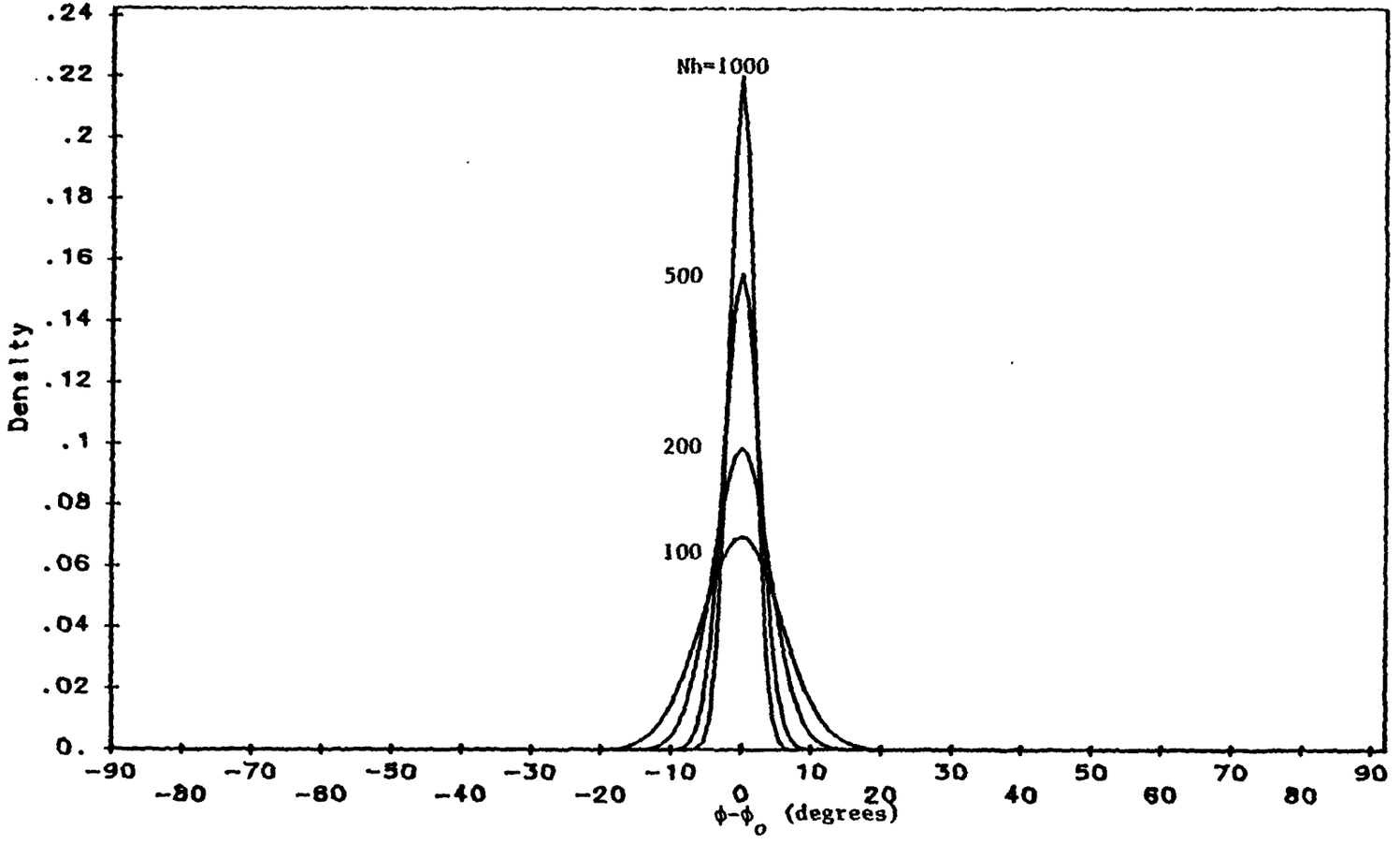

Figure 3-2: Probability Density of Estimator for Uncorrelated Noise; Nh=100,200,500,1000

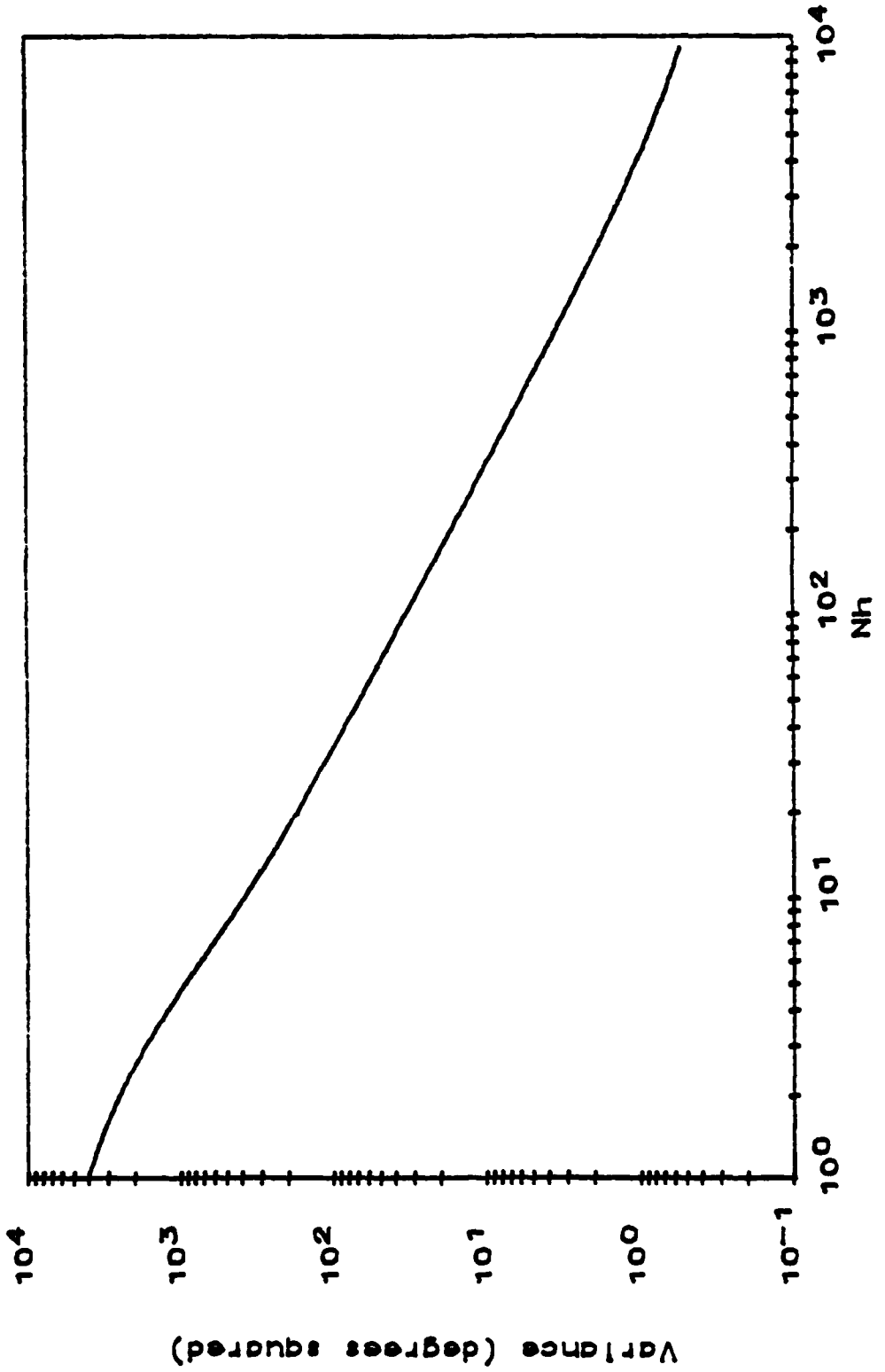

Figure 3-3: Variance of Estimator for Uncorrelated Noise

where the first integral is zero due to its odd integrand integrated over symmetric limits, and the second integral is 1 since it represents the area under density, $f(\phi)$. Hence, with this choice of integration limits, the mean is equal to the true value (i.e., the estimator is unbiased), so that the variance is a measure of the fluctuation of ϕ about the true value, ϕ_o.

The estimate of time delay is given by

$$\Delta\hat{\tau} = \frac{\phi}{\omega_o \hat{s}}$$

which has mean equal to the true value (if $\hat{s}=s$), and variance

$$E\{\Delta\hat{\tau}\} = \frac{\mu}{\omega_o \hat{s}} = \frac{\phi_o}{\omega_o \hat{s}}$$

$$\text{var}\{\Delta\hat{\tau}\} = \frac{1}{(\omega_o \hat{s})^2}\,\sigma^2 \quad ,$$

where $\sigma^2 = \text{var}(\phi)$ is shown in Figure 3-3.

From Figure 3-3, it is seen that the variance of this estimator decreases approximately as $1/Nh$. Under previously stated assumption, N can be replaced by the time-bandwidth product of the signal, and the time delay estimator is seen to take advantage of the processing gain of large time-bandwidth product signals to reduce the variance of the time difference estimate.

In order to test the validity of the variance curve of Figure 3-3, the estimation procedure of Figure 2-1 is simulated on a computer. The signal used for the simulation is based on a Welsh construction[17] with a real envelope. The signal is of the following form

$$f(t)e^{j2\pi f_o t}$$

where

f_o = 30,000Hz

$f(t) = w(t)\cos 2\pi f_i t \quad (i-1)T_s < t < iT_s$

T_s = subpulse length
= .05 seconds

w(t) = 50 dB Taylor Window[18]

i	f_i
1	550
2	750
3	650
4	700
5	350
6	850
7	600
8	400
9	500
10	450
11	800
12	300

The ambiguity function of this signal is shown in Figure 3-4. Note that this signal has good resolution both in τ and in s, due to its large time-bandwidth product. Note also that by giving the signal a real envelope, one obtains a symmetric spectrum as required by (2-6).

The signal is sampled at 1700Hz and matched-filtered using the correct τ amd s values, $\hat{\tau} = \tau_1 = 1.0$, $\hat{s} = s = 1$. Next, 1000 complex Gaussian noise samples were generated, normalized as in (3-9), and added

COSTAS CODE: TAYLOR WINDOW

REAL ENVELOPE ON TRANSMITTED SIGNAL

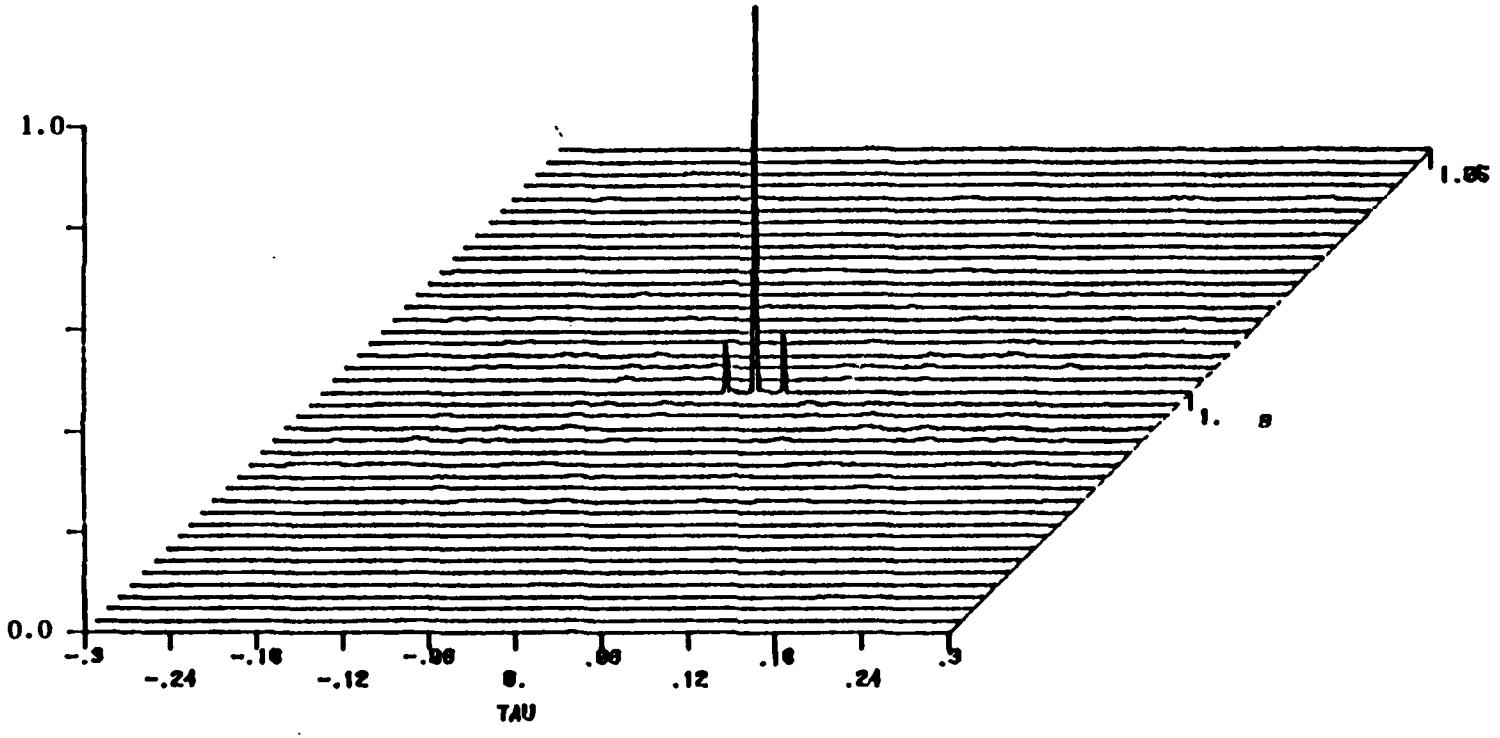

Figure 3-4: Ambiguity Function of Signal Used in Example

to Q as in (3-8) to obtain a sample mean and variance to compare with the theoretical unbiased mean and the variance of Figure 3-3. The results are summarized in Table 3-1 table for $\phi_o = 0$ and $\phi_o = 45°$.

Table 3-1

Theoretical versus Sample Means and Variances

	Nh	10	100	1000	10,000
$\phi_o = 0°$	Theoretical Mean (Deg)	0.000	0.000	0.000	0.000
	Sample Mean	0.068	0.045	0.015	0.005
	Theoretical Variance	380.0	33.2	3.3	0.36
	Sample Variance	369.0	34.0	3.4	0.34
$\phi_o = 45°$	Theoretical Mean	45.00	45.00	45.00	45.00
	Sample Mean	45.84	45.25	45.09	45.05
	Theoretical Variance	380.0	33.2	3.3	0.36
	Sample Variance	379.6	35.0	3.5	0.34

It is seen that the expressions derived above for the density function of the estimator generally predict variances consistent with the sample variances of the simulations even for values of Nh as low as 10, and the sample mean approaches the theoretical mean, ϕ_o, for large values of Nh.

This concludes the analysis of the estimator operating in uncorrelated noise. The next chapter will discuss the considerably more complicated case of noise which is correlated between channels.

CHAPTER 4

CORRELATED NOISE

In this chapter, the receiver performance is evaluated when operating in white Gaussian noise which is correlated between channels. As in the previous chapter, the noise is assumed to be a white, circularly complex Gaussian process, so that

$$E\{x_{ki}y_{ki}\} = 0 \qquad \text{for all } i;\ k = 1,2$$

$$E\{x_{ki}x_{kj}\} = E\{y_{ki}y_{kj}\} = \sigma_n^2\,\delta_{ij} \qquad k = 1,2.$$

The noise process is assumed to be correlated as follows:[6]

$$E\{x_{1i}x_{2j}\} = E\{y_{1i}y_{2j}\} = \rho\sigma_n^2\,\delta_{ij}$$

$$E\{x_{1i}y_{2j}\} = -E\{x_{2j}y_{1i}\} = \lambda\sigma_n^2\,\delta_{ij}.$$

A physical interpretation of ρ and λ is given in Appendix A. It is noted here for future reference that ρ and λ are such that

$$\rho^2 + \lambda^2 \leq 1. \tag{4-1}$$

This can be seen from examining eigenvalues of the covariance matrix for the density $f(x_1,y_1,x_2,y_2)$, noting that since the covariance matrix is positive definite, its eigenvalues must all be positive.[19]

The development of Chapter 3 may be followed up to (3-2) without modification. Equation (3-2) is repeated here for convenience:

$$\chi_k = \sqrt{E_o}\,e^{j\omega_o\hat{s}(\hat{\tau}-\tau_k)} \cdot \sum_i \hat{f}_i f_{ki} + \sum_i n_{ki}\hat{f}_i\, e^{-j\omega_o\hat{s}(t_i-\hat{\tau})} \qquad k = 1,2. \tag{4-2}$$

χ_k represents the output of the k^{th} summation block in Figure 2-1, and (4-2) assumes the correct time-stretch estimate. Since the complex noise is assumed correlated between channels, more care must be taken when absorbing the complex exponential of the last term of (4-2) into the noise process.

If the second term of (4-2) is written in terms of its real and imaginary components,

$$\sum_i n_{ki} \hat{f}_i \, e^{-j\omega_o \hat{s}(t_i - \hat{\tau})} = u_k + jv_k$$

then the correlation coefficients for u_1, v_1, u_2, v_2 can be expressed in terms of the input correlation coefficients, ρ and λ. Using the results of Appendix B and the fact that the time samples of the noise are independent, it can be shown that u_1, v_1, u_2, v_2 have the same correlation coefficients as x_{1i}, y_{1i}, x_{2i}, and y_{2i}; that is,

$$E\{u_1 u_2\} = E\{v_1 v_2\} = \rho\sigma_n^2$$

$$E\{u_1 v_2\} = -E\{u_2 v_1\} = \lambda\sigma_n^2 \, .$$

It is noted that the variances also remain unchanged, due to the fact that the processing signal is of unit energy.

As in the previous chapter, this processed noise term is denoted by η_k,

$$\eta_k = u_k + jv_k = \sum_i n_{ki} \hat{f}_i \, e^{-j\omega_o \hat{s}(t_i - \hat{\tau})} \qquad k = 1,2$$

with variance of real and imaginary parts equal to σ_n^2.

If A_k is again defined as

$$A_k = \sum_i \hat{f}_i f_{ki} \qquad k = 1,2,$$

then the output of each summation block in Figure 2-1 can be written as

$$X_k = \sqrt{E_o}\, A_k\, e^{j\omega_o \hat{s}(\hat{\tau}-\tau_k)} + \eta_k \qquad k = 1,2$$

so that the output Q, is given by

$$\begin{aligned} Q = X_1 X_2^* &= [\sqrt{E_o}A_1\, e^{j\omega_o \hat{s}(\hat{\tau}-\tau_1)} + \eta_1][\sqrt{E_o}A_2\, e^{-j\omega_o \hat{s}(\hat{\tau}-\tau_2)} + \eta_2^*] \\ &= E_o \cdot A_1 A_2 e^{j\omega_o \hat{s}(\tau_2-\tau_1)} + \sqrt{E_o}A_2\eta_1 e^{-j\omega_o \hat{s}(\hat{\tau}-\tau_2)} + \sqrt{E_o}A_1\eta_2^* e^{j\omega_o \hat{s}(\hat{\tau}-\tau_1)} \\ &\quad + \eta_1\eta_2^* \end{aligned} \tag{4-3}$$

Defining

$$\tilde{\eta}_1 = \eta_1 e^{-j\omega_o \hat{s}(\hat{\tau}-\tau_2)} = \tilde{u}_1 + j\tilde{v}_1$$

$$\tilde{\eta}_2 = \eta_2 e^{-j\omega_o \hat{s}(\hat{\tau}-\tau_1)} = \tilde{u}_2 + j\tilde{v}_2$$

it is again desired to find the correlation coefficients of $\tilde{u}_1$, $\tilde{v}_1$, $\tilde{u}_2$, $\tilde{v}_2$ in terms of ρ and λ. The results follow from direct application

of Appendix B, and are summarized below:

$$E\{\tilde{u}_1\tilde{u}_2\} = E\{\tilde{v}_1\tilde{v}_2\} = (c\rho - d\lambda)\sigma_n^2 = \tilde{\rho}\sigma_n^2$$

$$E\{\tilde{u}_1\tilde{v}_2\} = -E\{\tilde{v}_1\tilde{u}_2\} = (c\lambda + d\rho)\sigma_n^2 = \tilde{\lambda}\sigma_n^2$$

where

$$c = \cos \omega_o \hat{s}(\tau_2 - \tau_1)$$

$$d = \sin \omega_o \hat{s}(\tau_2 - \tau_1).$$

and the new correlation coefficients, $\tilde{\rho}$ and $\tilde{\lambda}$ are introduced to simplify notation in the following development. It is noted for future reference that

$$\tilde{\rho}^2 + \tilde{\lambda}^2 = (c^2 + d^2)(\rho^2 + \lambda^2)$$
$$= \rho^2 + \lambda^2 < 1$$

where $\rho^2 + \lambda^2 < 1$ as in (4-1).

Equation (4-3) can now be written in terms of $\tilde{\eta}_1$ and $\tilde{\eta}_2$ as

$$Q = E_o \cdot A_1 A_2 e^{j\omega_o \hat{s}(\tau_2 - \tau_1)} + \sqrt{E_o} A_2 \tilde{\eta}_1 + \sqrt{E_o} A_1 \tilde{\eta}_2^* + \tilde{\eta}_1 \tilde{\eta}_2^* e^{j\omega_o \hat{s}(\tau_2 - \tau_1)}$$

$$= E_o \cdot e^{j\omega_o \hat{s}(\tau_2 - \tau_1)} + \sqrt{E_o}(\tilde{\eta}_1 + \tilde{\eta}_2^*) + \tilde{\eta}_1 \tilde{\eta}_2^* e^{j\omega_o \hat{s}(\tau_2 - \tau_1)} , \qquad (4\text{-}4)$$

where the last step assumes that the estimate of time delay is correct, and that the time difference of arrival is small so that $A_1 = 1$ and $A_2 = 1$, as in the previous chapter.

Again, as a concession to tractability, conditions under which the last term is negligible are quantified. The expectation of the magnitude-squared of the process $\tilde{n}_1\tilde{n}_2^*$ can be found directly through tedious integration to be

$$E\{|\tilde{n}_1\tilde{n}_2^*|^2\} = E\{[Re(\tilde{n}_1\tilde{n}_2^*)]^2\} + E\{[Im(\tilde{n}_1\tilde{n}_2^*)]^2\}$$

$$4(1 + \tilde{\rho}^2 + \tilde{\lambda}^2) \leq 8\sigma_n^4$$

Where the inequality arises from the fact that $\tilde{\rho}^2 + \tilde{\lambda}^2 \leq 1$. Thus with the input signal-to-noise ratio defined as

$$h = \frac{E_o}{2N\sigma_n^2} ,$$

the ratio of the magnitude-squared of the first term of (4-4) to that of the second or third term has expectation

$$\frac{E_o^2}{E\{(\sqrt{E_o}\tilde{n}_k)^2\}} = Nh \qquad (4-5)$$

as in (3-6), while the ratio of the magnitude-squared of the first term to the expected magnitude-squared of the last term is

$$\frac{E_o^2}{E\{|\tilde{n}_1\tilde{n}_2|^2\}} \geq \frac{E_o^2}{8\sigma_n^4} = \frac{1}{8}\left(\frac{E_o}{\sigma_n^2}\right)^2 = \frac{1}{2}(Nh)^2 \qquad (4-6)$$

From (4-5) and (4-6) it is seen that the last term of (4-4) is again of second order, becoming negligible for large values of Nh. For example, if Nh = 1000, then the second and third terms are 30dB below the first,

while the last term is at least 57dB below the first. Throughout the rest of the chapter, the last term of (4-4) is dropped.

In terms of its real and imaginary parts, Q can be written as

$$Q = E_o \cdot e^{j\omega_o \hat{s}(\tau_2-\tau_1)} + \sqrt{E_o}\eta_1 + \sqrt{E_o}\eta_2^*$$

$$= E_o \cdot e^{j\phi_o} + \sqrt{E_o}\eta_1 + \sqrt{E_o}\eta_2^*$$

$$= a + jb + \sqrt{E_o}[\tilde{u}_1 + \tilde{u}_2 + j(\tilde{v}_1 - \tilde{v}_2)]$$

$$= a + \sqrt{E_o}(\tilde{u}_1 + \tilde{u}_2) + j[b + \sqrt{E_o}(\tilde{v}_1 - \tilde{v}_2)]$$

where

$$\phi_o = \omega_o \hat{s}(\tau_2 - \tau_1)$$

$$a = E_o \cos\phi_o \qquad b = E_o \sin\phi_o$$

$$\tilde{u}_1 = \mathrm{Re}\{\tilde{\eta}_1\} \qquad \tilde{v}_1 = \mathrm{Im}\{\tilde{\eta}_1\}$$

$$\tilde{u}_2 = \mathrm{Re}\{\tilde{\eta}_2\} \qquad \tilde{v}_2 = \mathrm{Im}\{\tilde{\eta}_2\}$$

$$\mathrm{var}\{\tilde{u}_k\} = \sigma_n^2 \qquad \mathrm{var}\{\tilde{v}_k\} = \sigma_n^2 \qquad k = 1,2$$

$$E\{\tilde{u}_1\tilde{u}_2\} = E\{\tilde{v}_1\tilde{v}_2\} = \tilde{\rho}\,\sigma_n^2$$

$$E\{\tilde{u}_1\tilde{v}_2\} = -E\{\tilde{v}_1\tilde{u}_2\} = \tilde{\lambda}\,\sigma_n^2$$

$$\tilde{\rho} = \rho\cos\phi_o - \lambda\sin\phi_o$$

$$\tilde{\lambda} = \rho\sin\phi_o + \lambda\cos\phi_o\ .$$

The estimate of ϕ_o is then given by ϕ, where

$$\phi = \tan^{-1}\left(\frac{b + \sqrt{E_o}(\tilde{v}_1 - \tilde{v}_2)}{a + \sqrt{E_o}(\tilde{u}_1 + \tilde{u}_2)}\right) = \tan^{-1}\left(\frac{b + y}{a + x}\right) ,$$

and where $x \equiv \tilde{u}_1 + \tilde{u}_2$, $y \equiv \tilde{v}_1 - \tilde{v}_2$. In order to evaluate the statistics of this estimator, it is necessary to find the covariance matrix for the numerator and denominator of the argument of the arctangent. Denoting this by $\underline{R}_{xy}$, it is seen that

$$\underline{R}_{xy} = \begin{vmatrix} \overline{E\{x^2\}} & \overline{E\{xy\}} \\ \underline{E\{xy\}} & E\{y^2\} \end{vmatrix} = 2E_o \cdot \sigma_n^2 \begin{vmatrix} \overline{(1 + \tilde{\rho})} & -\tilde{\lambda} \\ -\tilde{\lambda} & (1 - \tilde{\rho}) \end{vmatrix}$$

$$= \begin{vmatrix} \overline{\sigma_x^2} & \rho_{xy}\sigma_x\sigma_y \\ \rho_{xy}\sigma_x\sigma_y & \sigma_y^2 \end{vmatrix}$$

where

$$\sigma_x^2 = 2E_o \cdot \sigma_n^2(1 + \tilde{\rho})$$

$$\sigma_y^2 = 2E_o \cdot \sigma_n^2(1 - \tilde{\rho})$$

$$\rho_{xy} = \frac{-\tilde{\lambda}}{\sqrt{1-\tilde{\rho}^2}} .$$

It is noted that $\rho_{xy} < 1$ since $\tilde{\rho}^2 + \tilde{\lambda}^2 < 1$. The joint Gaussian density is then[8]

$$f(x,y) = \frac{1}{2\pi|\underline{R}_{xy}|^{1/2}} \exp\left(-\frac{1}{2}[x,y]\,\underline{R}_{xy}^{-1}\begin{vmatrix} x \\ y \end{vmatrix}\right)$$

$$= \frac{1}{2\pi\sigma_x\sigma_y\sqrt{1-\rho_{xy}^2}} \exp\left[\frac{-1}{2(1-\rho_{xy}^2)}\left(\frac{x^2}{\sigma_x^2} - 2\rho_{xy}\frac{xy}{\sigma_x\sigma_y} + \frac{y^2}{\sigma_y^2}\right)\right] .$$

Once again, the change of variables $x + a = r\cos\phi$, $y + b = r\sin\phi$ is made to obtain the density for $\phi = \tan^{-1}\left(\frac{y+b}{x+a}\right)$. After considerable algebraic manipulation the joint density $f(r,\phi)$ is obtained:

$$f(r,\phi) = \frac{r}{2\pi\sigma_x\sigma_y\sqrt{1-\rho_{xy}^2}} e^{-k}\, e^{-\mu\left(\frac{r}{E_o}\right)^2 + 2\nu\left(\frac{r}{E_o}\right)}$$

where

$$k = \frac{1}{2(1-\rho_{xy}^2)}\left[\frac{a^2}{\sigma_x^2} + \frac{b^2}{\sigma_y^2} - 2\rho_{xy}\frac{ab}{\sigma_x\sigma_y}\right]$$

$$\mu = \frac{E_o^2}{2(1-\rho_{xy}^2)}\left[\frac{\cos^2\phi}{\sigma_x^2} + \frac{\sin^2\phi}{\sigma_y^2} - 2\rho_{xy}\frac{\sin\phi\cos\phi}{\sigma_x\sigma_y}\right]$$

$$\nu = \frac{E_o}{2(1-\rho_{xy}^2)}\left[\frac{a\cos\phi}{\sigma_x^2} + \frac{b\sin\phi}{\sigma_y^2} + \rho_{xy}\left(\frac{a\sin\phi + b\cos\phi}{\sigma_x\sigma_y}\right)\right].$$

The desired density, $f(\phi)$ is again obtained by integrating the joint density, $f(r,\phi)$ over all values of r, i.e.

$$f(\phi) = \int_0^\infty f(r,\phi)dr.$$

This integral is of the same form as that of (3-11), but with considerably more complicated coefficients in the exponential. These coefficients can be substantially simplified by writing σ_x, σ_y and ρ_{xy} in

terms of σ_n, $\tilde{\rho}$, and $\tilde{\lambda}$ and by recalling that $a = E_o\cos\phi_o$ and $b = E_o\sin\phi_o$, yielding

$$k = \frac{E_o}{4\sigma_n^2(1-\tilde{\rho}^2-\tilde{\lambda}^2)}\left[1 - \tilde{\rho}\cos(2\phi_o) + 2\,\tilde{\lambda}\cos\phi_o\sin\phi_o\right]$$

$$\mu = \frac{E_o}{4\sigma_n^2(1-\tilde{\rho}^2-\tilde{\lambda}^2)}\left[1 - \tilde{\rho}\cos(2\phi) + 2\,\tilde{\lambda}\cos\phi\sin\phi\right]$$

$$\nu = \frac{E_o}{4\sigma_n^2(1-\tilde{\rho}^2-\tilde{\lambda}^2)}\left[\cos(\phi-\phi_o) - \tilde{\rho}\cos(\phi+\phi_o) + \tilde{\lambda}\sin(\phi+\phi_o)\right]. \quad (4\text{-}7)$$

The density is then written

$$f(\phi) = \frac{e^{-k}}{4\pi E_o\sigma_n^2\sqrt{1-\tilde{\rho}^2-\tilde{\lambda}^2}}\int_o^\infty r\,\exp\left[-\mu\left(\frac{r}{E_o}\right)^2 + 2\nu\left(\frac{r}{E_o}\right)\right]dr$$

$$= \frac{E_o e^{-k}}{4\pi\sigma_n^2\sqrt{1-\tilde{\rho}^2-\tilde{\lambda}^2}}\int_o^\infty r\,\exp\left[-\mu\,r^2 + 2\nu r\right]dr \quad (4\text{-}8)$$

Where the second line results from a change of integration variable. Once again the integral for $f(\phi)$ cannot be put in closed form. It is seen that for the correlated noise case, the density $f(\phi)$ is a rather unwieldy function of several parameters: E_o/σ_n^2, $\tilde{\rho}$, $\tilde{\lambda}$, and ϕ_o. In addition, $\tilde{\rho}$ and $\tilde{\lambda}$ are in turn functions of ϕ_o and the input noise correlation coefficients ρ and λ. The quantity E_o/σ_n^2 in (4-7) and (4-8)

is replaced by the quantity 2Nh to get the density in terms of the input signal-to-noise ratio.

Roughly speaking, the quantity E_o/σ_n^2 controls the sharpness of the density, while the correlation coefficients alter its shape. The density is integrated numerically for various combinations of parameters yielding Figures 4-1, 4, 7, and 10.

The densities are then used to generate curves of the mean and variance of the estimator for these combinations of parameters, yielding the continuous curves in Figures 4-2, 5, 8, 11 and 4-3, 6, 9, 12. It is again noted that the moment quantities depend on the integration limits chosen. For the correlated noise case, the choice of these limits does not seem as clear as it was for the uncorrelated noise case, because the estimator is now biased. If the same limits are chosen for this case however, the estimator will become unbiased for large values of Nh, so the integration limits are again chosen as $\phi_o - \pi \leq \phi \leq \phi_o + \pi$.

These curves are again verified using the same signal and sampling parameters as in the previous chapter, yielding the discrete points in the mean and variance curves. The noise model used in these simulations is described in Appendix A, with the incoherent noise correlation coefficient, ρ_i set equal to zero so that the incoherent noise is uncorrelated between channels. The coherent noise is the same in each channel except for a phase delay,

$$n_{2i}^c = e^{-j\phi_c} n_{1i}^c$$

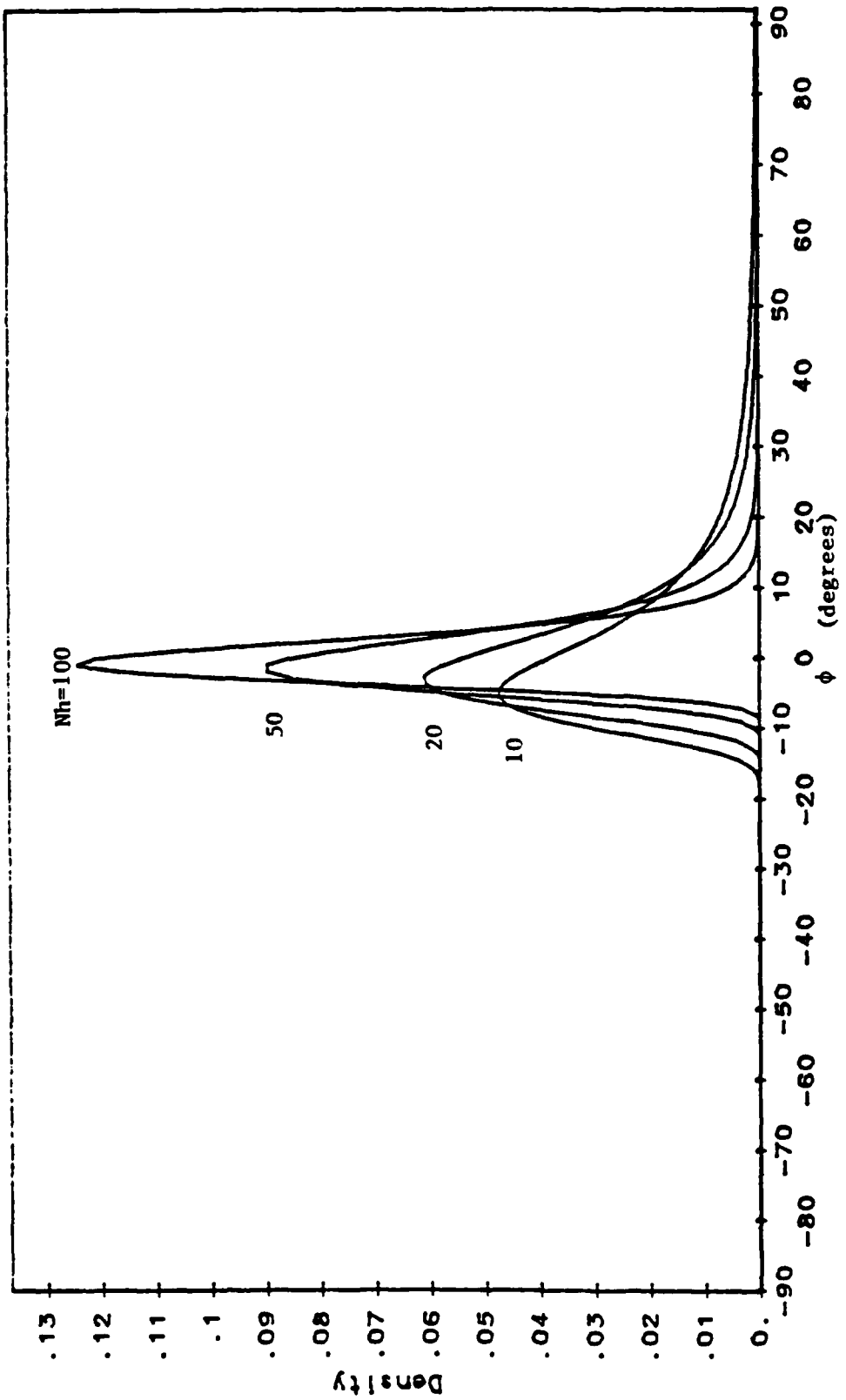

Figure 4-1: Probability Density of Estimator; ρ=.67, λ=.67, ϕ_o=0

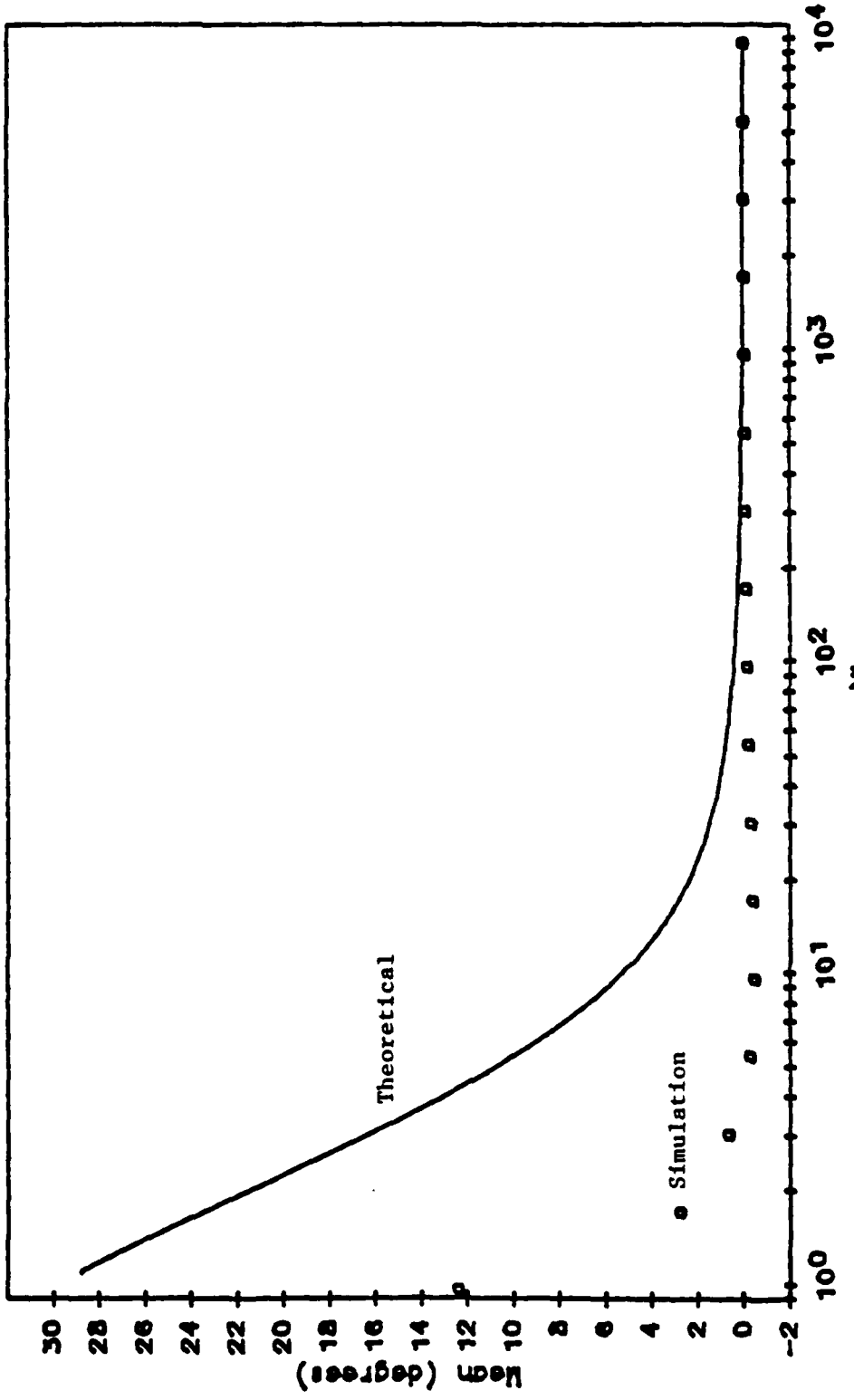

Figure 4-2: Mean of Estimator; ρ=.67, λ=.67, ϕ_o=0

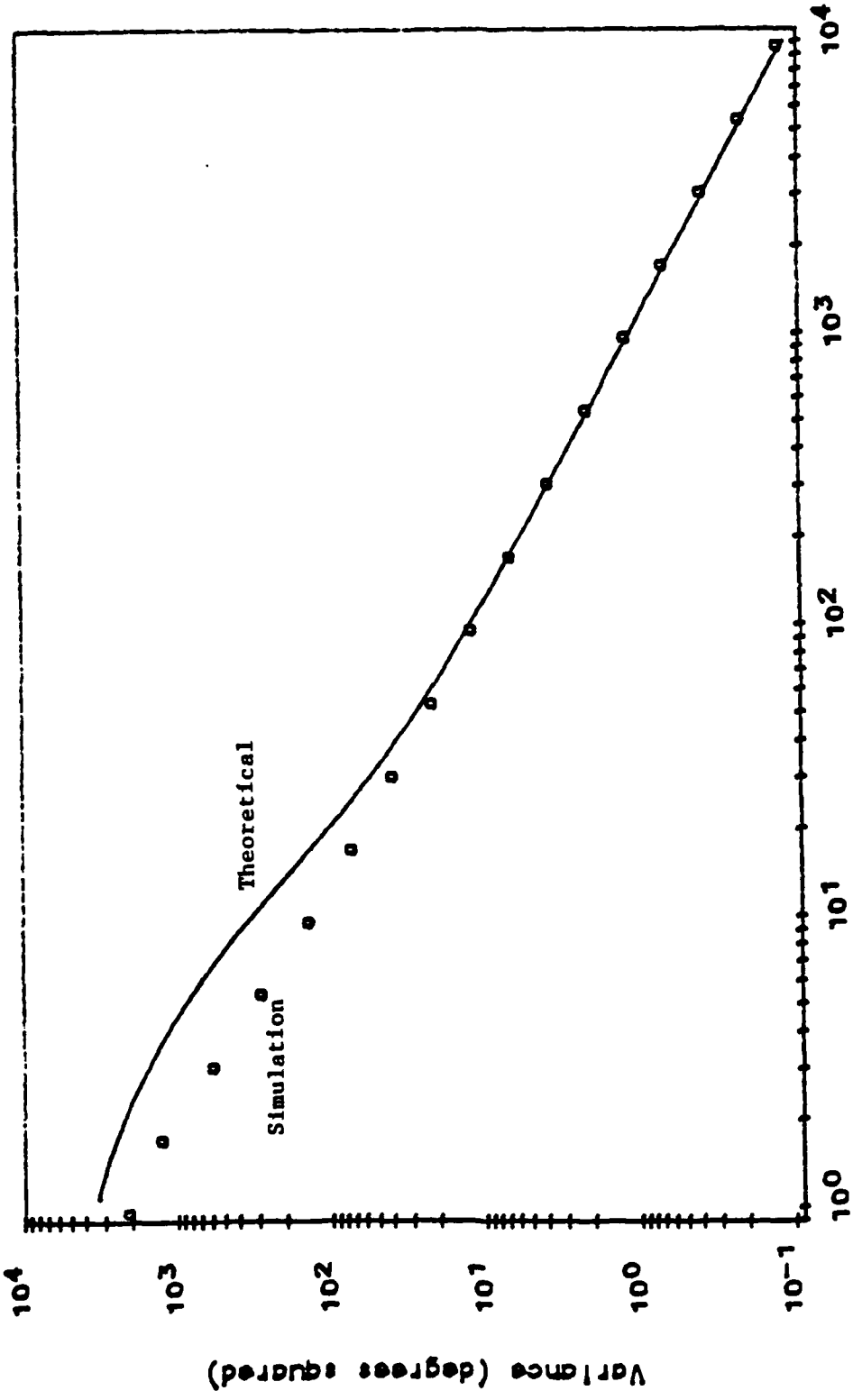

Figure 4-3: Variance of Estimator; ρ=.67, λ=.67, ϕ_o=0

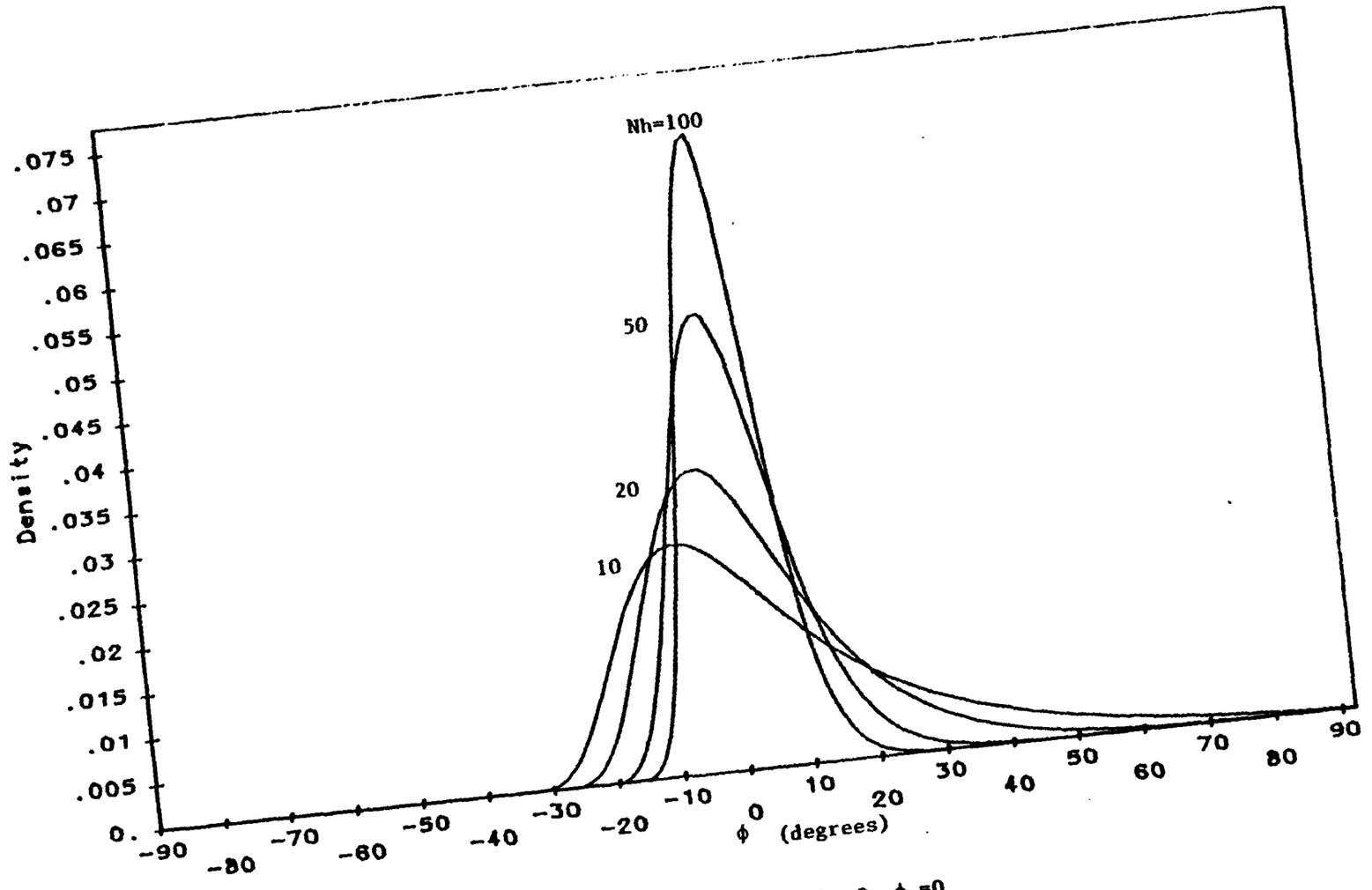

Figure 4-4: Probability Density of Estimator; ρ=0, λ=.9, ϕ_o=0

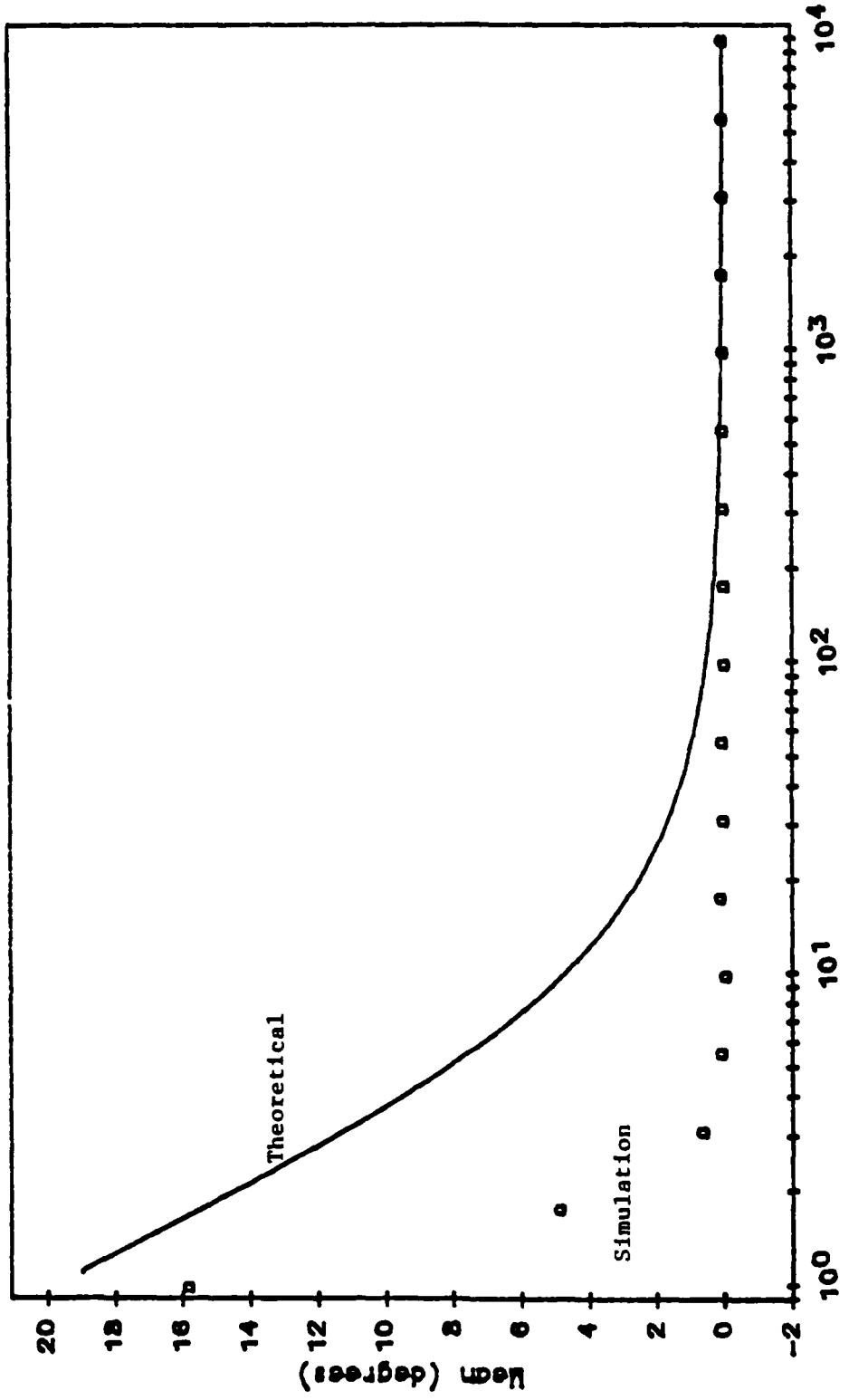

Figure 4-5: Mean of Estimator; ρ=0, λ=.9, ϕ_o=0

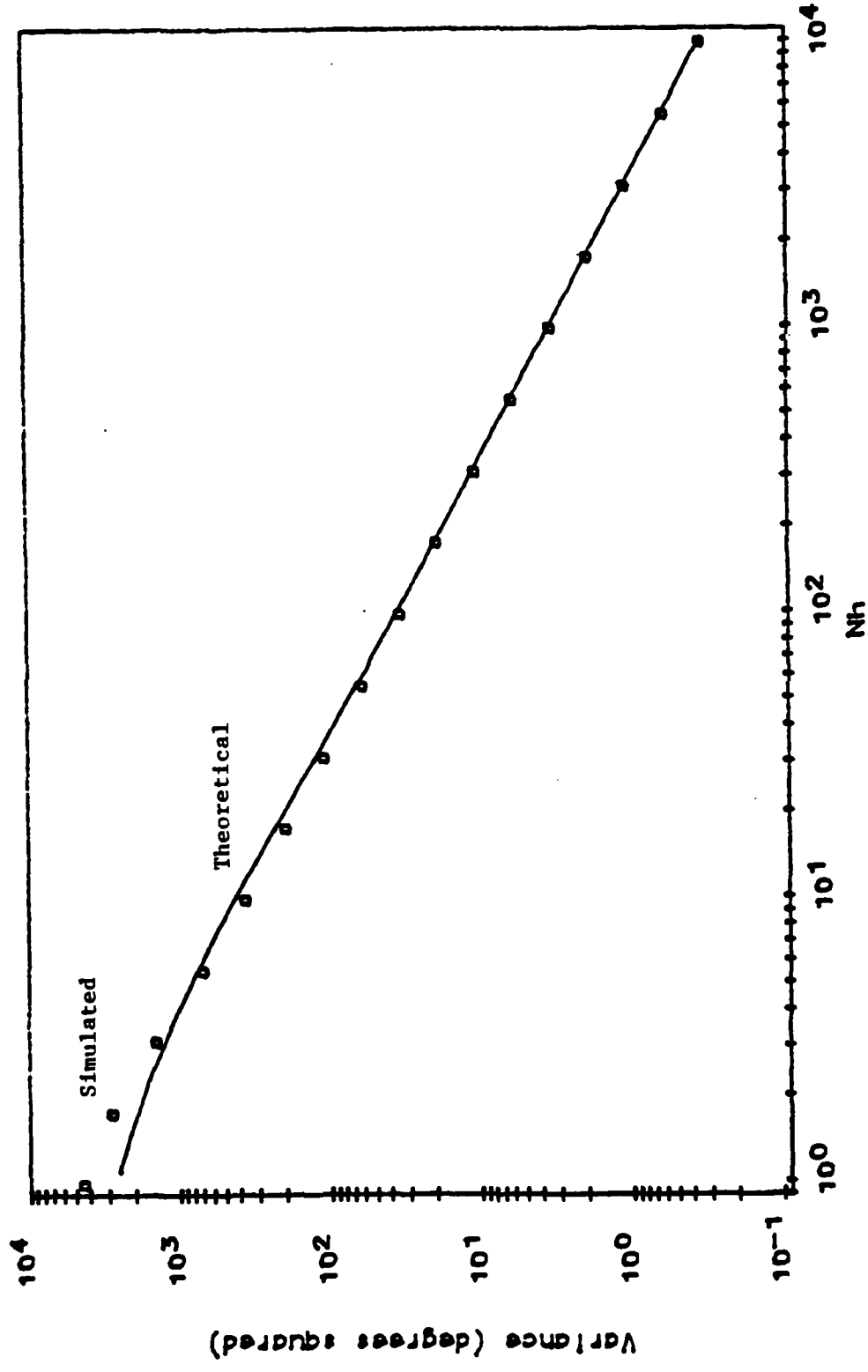

Figure 4-6: Variance of Estimator; $\rho=0$, $\lambda=.9$, $\phi_o=0$

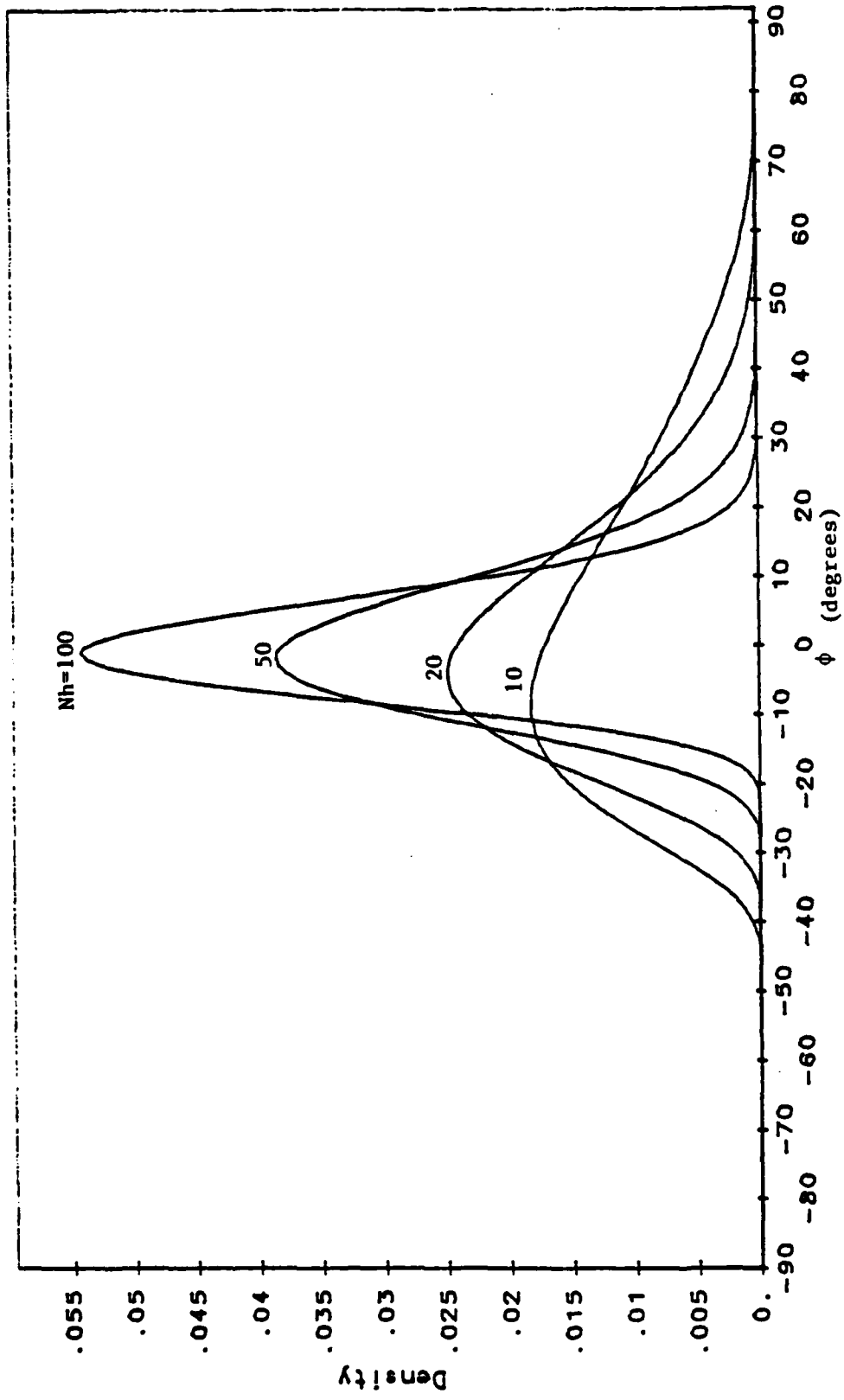

Figure 4-7: Probability Density of Estimator; ρ=-.67, λ=.67, ϕ_o=0

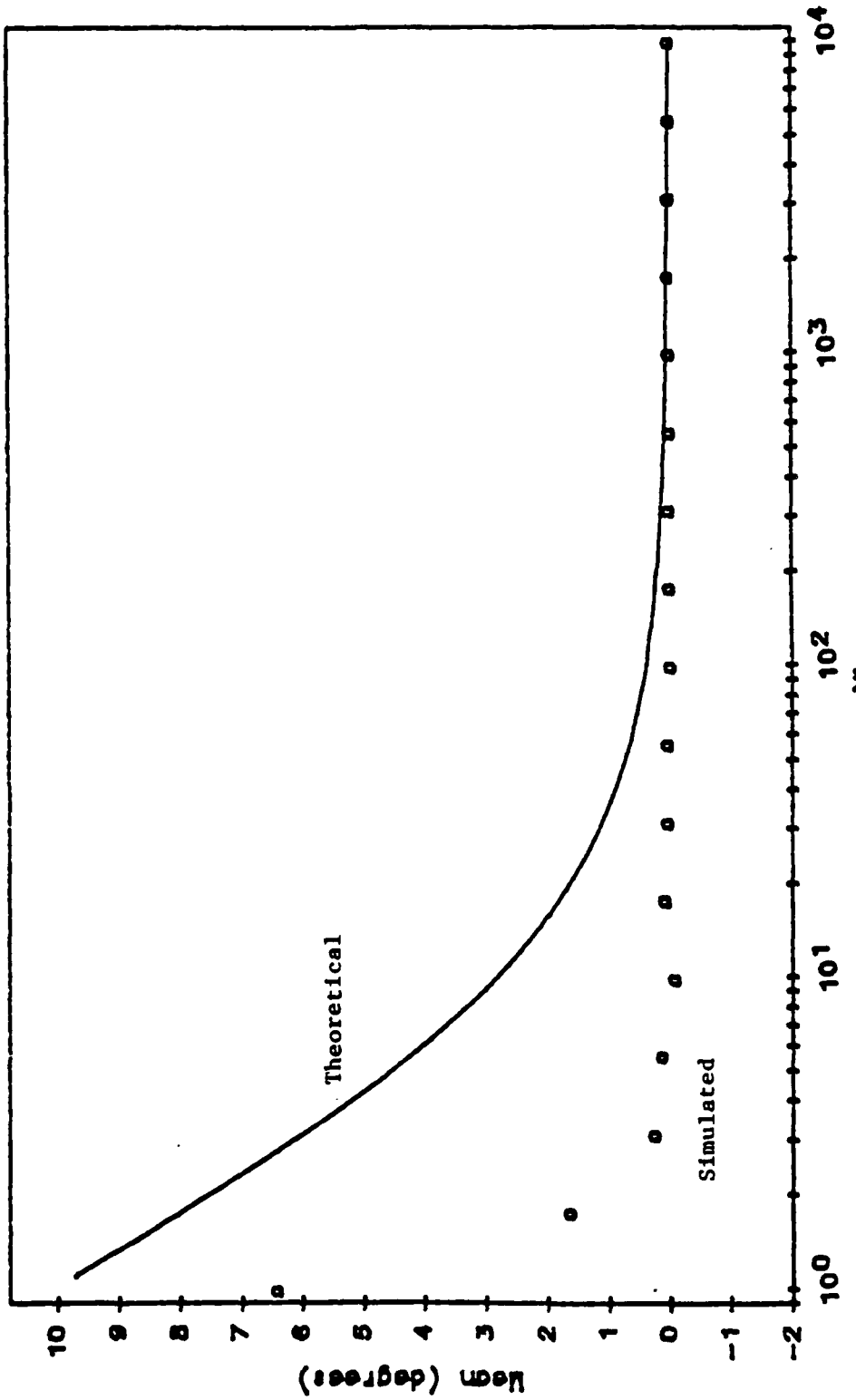

Figure 4-8: Mean of Estimator; ρ=-.67, λ=.67, ϕ_o=0

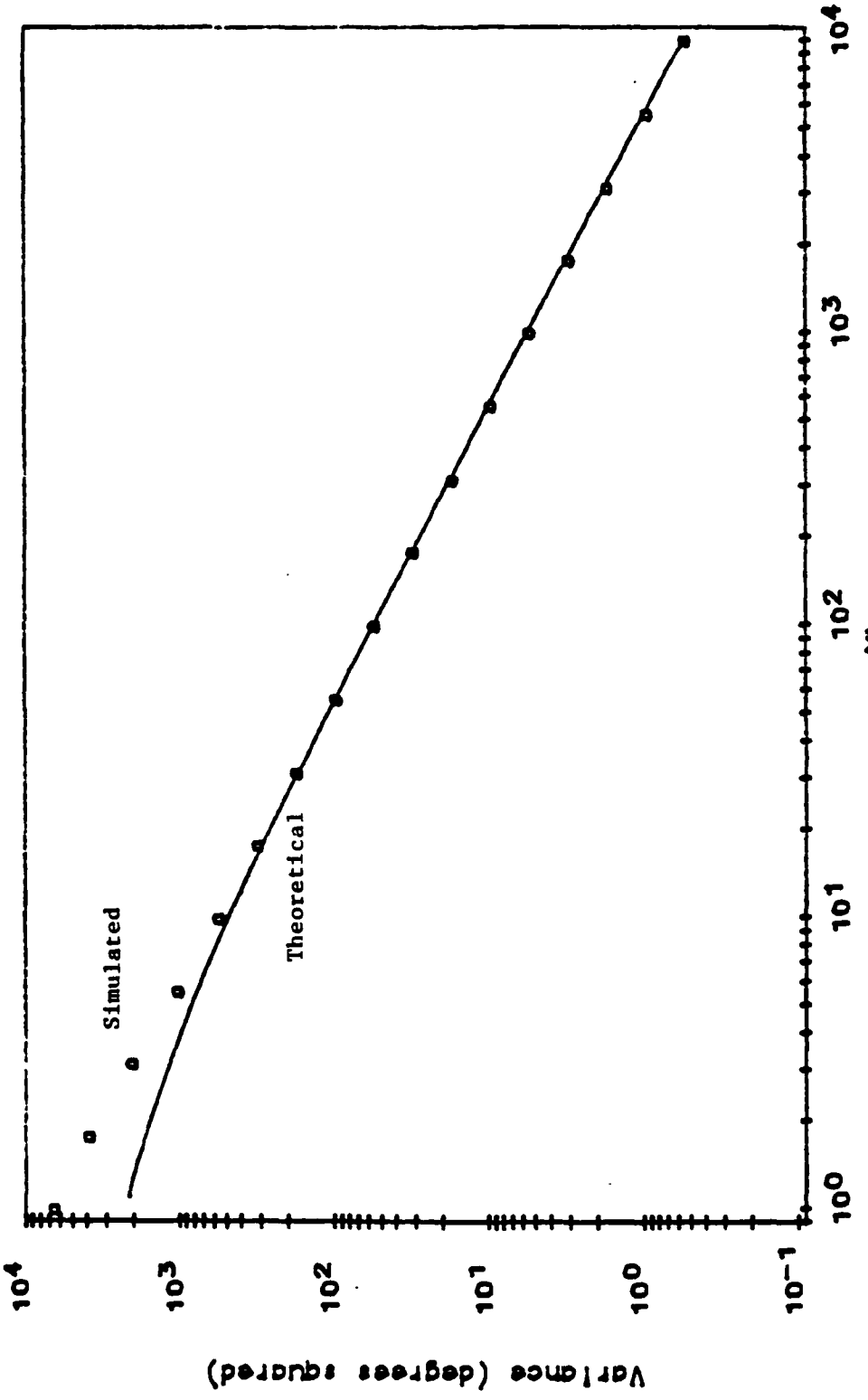

Figure 4-9: Variance of Estimator; ρ=-.67, λ=.67, ϕ_o=0

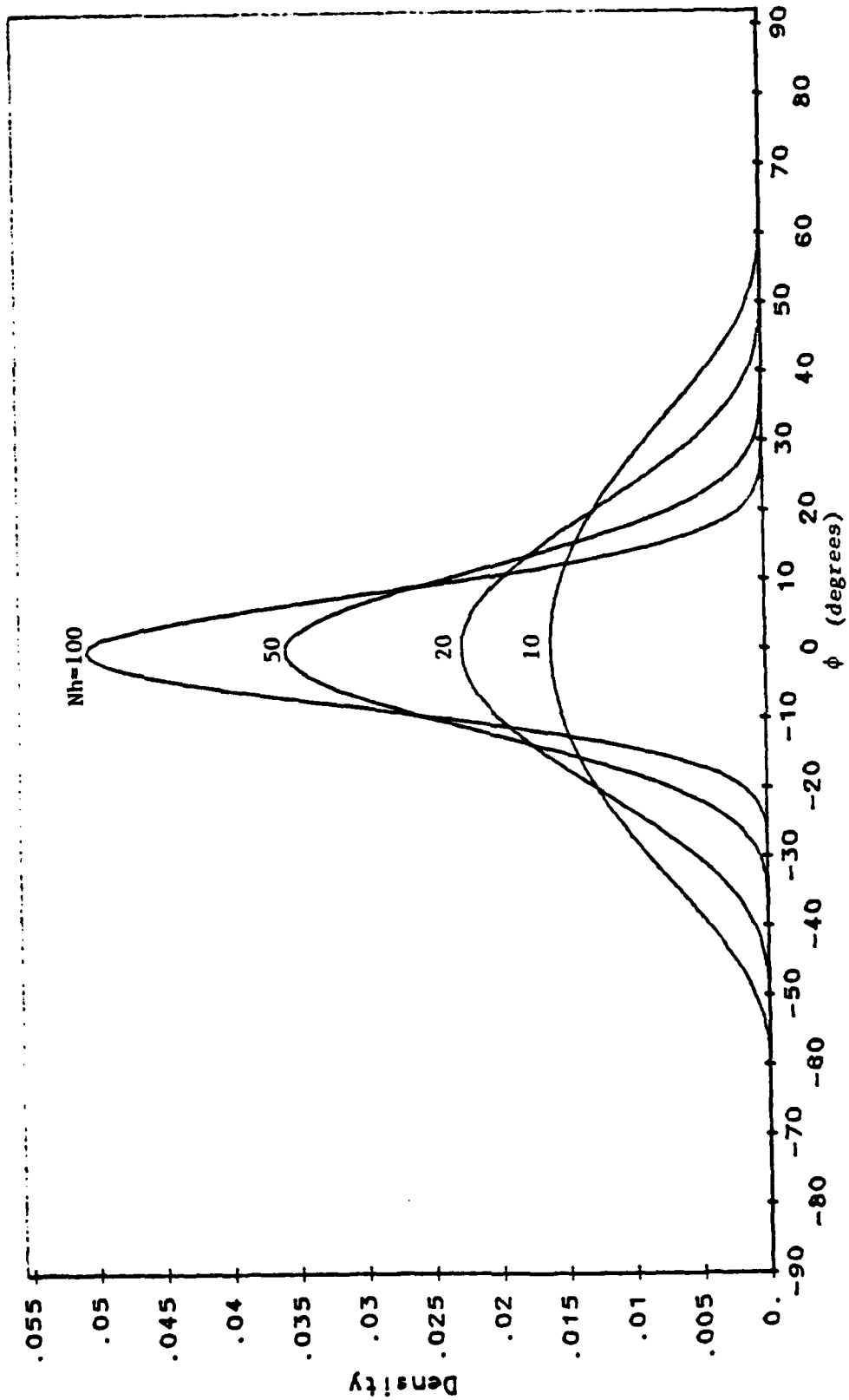

Figure 4-10: Probability Density of Estimator; ρ=-.9, λ=0, ϕ_o=0

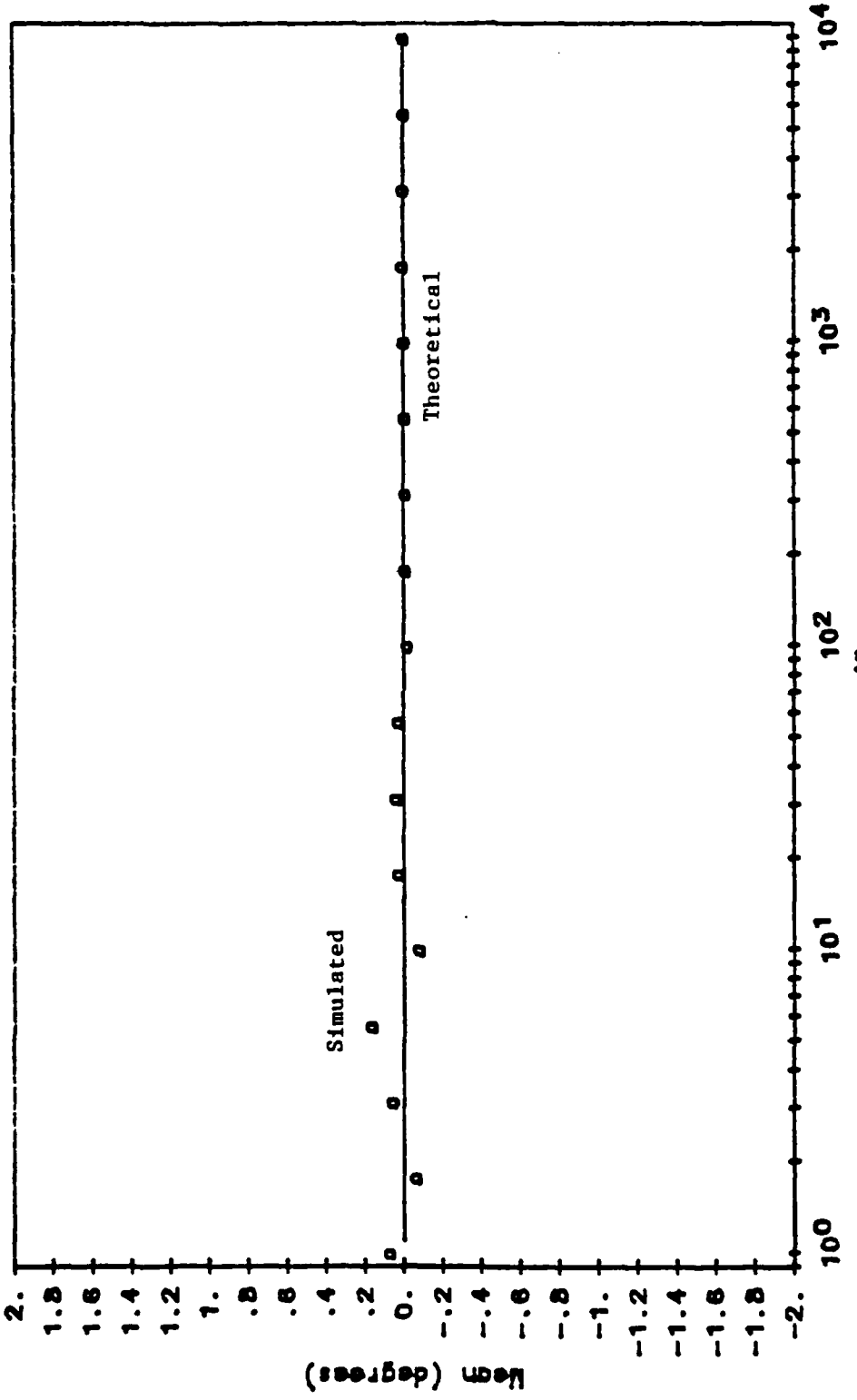

Figure 4-11: Mean of Estimator; ρ=-.9, λ=0, ϕ_o=0

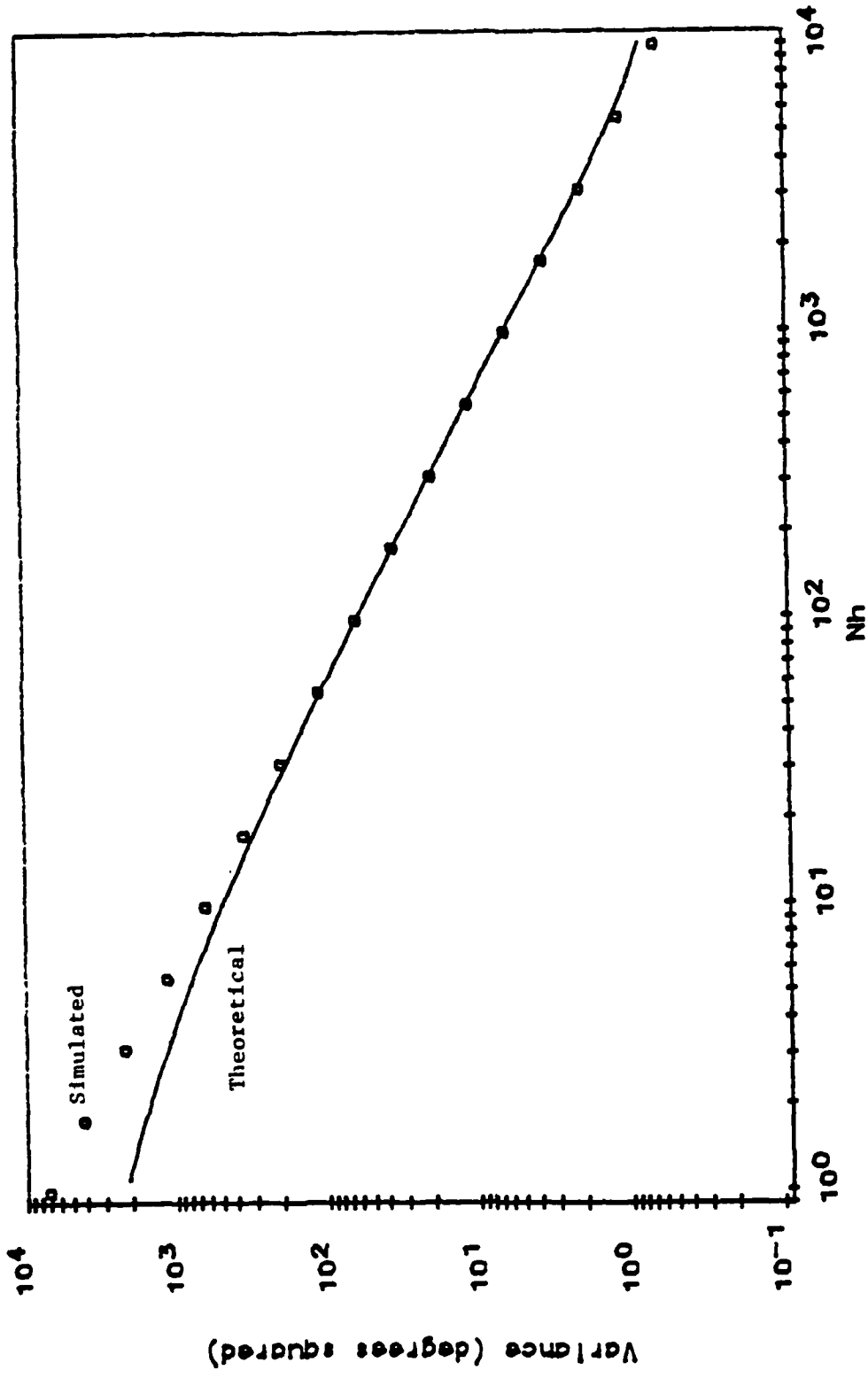

Figure 4-12: Variance of Estimator; ρ=-.9, λ=0, ϕ_o=0

where $\phi_c = \tan^{-1}(\frac{\lambda}{\rho})$, ρ and λ being the input noise correlation coefficents. The incoherent noise has variance of real and imaginary parts

$$\sigma_i^2 = (1-r)\sigma_n^2,$$

while the coherent noise has variance

$$\sigma_c^2 = r\sigma_n^2,$$

where $r = \sqrt{\rho^2+\lambda^2}$, and σ_n^2 is the total noise variance.

From these figures, it is seen that both the sample and theoretical means approach the true values for large values of Nh. Also, the variances predicted by theory are consistent with the sample variances generated by the simulation for large Nh. The theoretical curves are accurate only for Nh of about 100 or greater due to the approximation made by developing the last term of 4-4.

Again it is seen that for large Nh, the variance drops of as 1/Nh. Replacing N with the time-bandwidth product of the signal (as in the previous chapter), it is again seen that the estimator takes advantage of the processing gain of large time-bandwidth signals to reduce the estimator variance.

The analysis of this and the previous chapters has assumed that the time-stretch and -delay estimates are correct. In most cases these estimates will not be exactly correct. The effect of a τ-s mismatch is the subject of the following chapter.

CHAPTER 5

τ-s MISMATCH

In Chapters 3 and 4 it was assumed that the estimates of time-delay and -stretch were correct. In practice, these estimates will not be exact, and this will affect the performance of the time difference estimator. In order to examine the effects of a τ-s mismatch, it is necessary to go back to Equation (3-2), before any assumptions about $\hat{\tau}$ and $\hat{s}$ were made. The second line of (3-2) is repeated here for convenience:

$$\chi_k = \sqrt{E_o} \cdot \sum_i \hat{f}_i f_{ki} \, e^{j\omega_o[(\hat{s}-s)t_i + \hat{s}\hat{\tau} - s\tau_k]} + \sum_i n_{ki} \, \hat{f}_i \, e^{-j\omega_o \hat{s}(t_i - \hat{\tau})}$$

where χ_k represents the output of the k^{th} channel in Figure 2-1. This can be rewritten in the following form:

$$\chi_k = \sqrt{E_o} e^{j\omega_o s(\hat{\tau}-\tau_k)} \, e^{-j\omega_o(s-\hat{s})\hat{\tau}} \cdot \sum_i \hat{f}_i f_{ki} \, e^{j\omega_o(s-\hat{s})t_i} + \eta_k$$

$$= \sqrt{E_o} e^{j\phi_k} \, e^{j\beta} \sum_i \hat{f}_i f_{ki} \, e^{j\alpha_i} + \eta_k$$

where

$$\phi_k = \omega_o s(\hat{\tau}-\tau_k)$$

$$\alpha_i = \omega_o(s-\hat{s})t_i \, , \quad \beta = \omega_o(s-\hat{s})\hat{\tau}$$

$$\eta_k = \sum_i n_{ki} \, \hat{f}_i \, e^{-j\omega_o \hat{s}(t_i - \hat{\tau})}$$

The output of Figure 2-1 is then written as

$$Q = X_1 X_2^* = E_o \cdot e^{j\phi_o} e^{j(\beta-\beta)} \sum_i \hat{f}_i f_{1i} e^{j\alpha_i} \sum_j \hat{f}_j^* f_{2j}^* e^{-j\alpha_j}$$

$$+ \sqrt{E_o} e^{-j\phi_2} e^{-j\beta} \eta_1 \sum_j \hat{f}_j^* f_{2j}^* e^{-j\alpha_i} + \sqrt{E_o} e^{j\phi_1} e^{j\beta} \eta_2^* \sum_i \hat{f}_i f_{1i} e^{j\alpha_i}$$

$$+ \eta_1 \eta_2^* \qquad (5\text{-}2)$$

where

$$\phi_o = \phi_1 - \phi_2 = \omega_o s(\tau_2 - \tau_1) \quad .$$

In this equation, $e^{j\phi_o}$ represents the true signal phase difference, and it is seen that the bias represented by the factor $e^{j\beta}$ cancels itself, so that the only bias remaining in the first term is that contributed by the double summation. It is also noted that the factors $e^{\pm j\beta}$ and $e^{\pm j\alpha_i}$ do not affect the correlation coefficients between the second and third terms (see Appendix B). The last term will be dropped under previously stated SNR assumptions.

If the assumption is again made that the time difference of arrival, $\tau_2 - \tau_1$ is small relative to the bandwidth of the signal as in previous chapters, then $f_{2i} \approx f_{1i}$, so that the first term in (5-2) becomes

$$E_o \cdot e^{j\phi_o} \sum_i \hat{f}_i f_{1i} e^{j\alpha_i} \cdot \sum_j \hat{f}_j^* f_{2j}^* e^{-j\alpha_j} \approx E \cdot e^{j(\phi_1 - \phi_2)} \left| \sum_i \hat{f}_i f_{1i} e^{j\alpha_i} \right|^2 , \qquad (5\text{-}3)$$

so that there is no bias in the estimate of ϕ_o due to an incorrect time-stretch hypothesis. There still remains, however, a bias in the time difference estimate. This bias occurs from using the estimated time stretch, $\hat{s}$, rather than the true time-stretch, s. The estimated time difference (in the absence of noise) is

$$\Delta\hat{\tau} = \frac{\phi_o}{\omega_o\hat{s}} = \frac{\phi_o}{\omega_o s + \omega_o(s-\hat{s})} = \frac{\phi}{\omega_o s}\left(1 - \frac{s-\hat{s}}{s}\right) = \Delta\tau\left(1 - \frac{s-\hat{s}}{s}\right) \quad (5\text{-}4)$$

where $\Delta\hat{\tau}$ is the estimate of $\tau_2-\tau_1$, $\Delta\tau$ is the true value, $\phi_o = \phi_1-\phi_2 = \omega_o s(\tau_2-\tau_1)$, and where a binomial expansion yields the approximation. For reasonably good time-stretch estimates (i.e., $|s-\hat{s}|<<1$) this bias will be negligible.

Comparing the magnitude-squared factor in (5-3) with (2-3) and noting the discussion following (2-3) it is seen that this factor is the magnitude-squared of the matched filter output whose main peak is at $\hat{\tau} = \tau_1$, $\hat{s} = s$, evaluated at the point $(\hat{\tau},\hat{s})$ corresponding to the estimates of the the true values. If the τ and s estimates are not exactly correct, the magnitude-squared factor in (5-3) will become smaller, effectively lowering the signal-to-noise ratio.

Thus, it is seen that a τ-s mismatch does not affect the noise terms (or change any bias due to the noise terms), and if the time difference of arrival is small, the only effect is a slight bias represented by (5-4), and a decrease in the signal-to-noise ratio due to the magnitude-squared factor in (5-3).

If the time difference of arrival cannot be assumed small, as was necessary to derive (5-3), then the sum must remain as in the first term of (5-2). The problem thus becomes more difficult, and the performance depends on the particular signal employed.

A special case of interest here is that of a real envelope signal (such as that employed in the examples of the previous two chapters). In this case, the double sum in first term of (5-2) can be written as follows:

$$\sum_i \hat{f}_i f_{1i}\, e^{j\alpha_i} \sum_j \hat{f}_j^* f_{2j}^*\, e^{-j\alpha_j} = \sum_i \sum_j \hat{f}_i f_{1i}\, \hat{f}_j^* f_{2j}^*\, e^{j\omega_o(s-\hat{s})(t_i-t_j)} \tag{5-5}$$

(where the complex conjugate symbols have been retained for future reference) so that a crude upper bound can be placed on the phase bias contributed by this term:

$$|\phi_b| < \omega_o |s-\hat{s}| T \tag{5-6}$$

where ϕ_b denotes the phase bias and T is the signal duration.

It is desired to obtain an idea of the typical size of the estimation errors for the time-stretch. The estimation errors for matched filter receivers have been considered by VanTrees[10] and by Cook and Bernfeld[11], who use a Cramér-Rao lower bound approach to derive an expression for the minimum error variances for this estimate, and who show that the estimation errors approach the Cramér-Rao bound for maximum-likelihood estimators.

In general, the estimation error for s will be coupled with that for τ, but a sufficient condition under which these estimates become uncoupled is that the signal employed has a real envelope[10], which has already been assumed.

Adapting the discussion in Cook and Bernfeld, and noting equation (2-2), the variance for the time-stretch estimate is bounded as follows:

$$E\{(s-\hat{s})^2\} > \frac{(1/\omega_o)^2}{\xi^2 h} \qquad (5\text{-}7)$$

where h is the input SNR, and ξ is the RMS signal duration, given by

$$\xi^2 = \frac{1}{E} \int_{-T/2}^{T/2} t^2 |f(t)|^2 dt$$

where E is the signal energy, and f(t) is the unsampled signal envelope. Following the example given in the paper by Ricker,[7] if the real envelope has constant amplitude, w_o, and bandwidth $B >> \frac{1}{T}$, the energy becomes

$$E = \frac{1}{2} w_o^2 T$$

and

$$\xi^2 = \frac{2}{w_o^2 T} \int_{-T/2}^{T/2} w_o^2 t^2 dt = \frac{T^2}{6}$$

so that

$$E\{(s-\hat{s})^2\} > \frac{6}{(\omega_o T)^2 h} \qquad (5\text{-}8)$$

If the standard deviation corresponding to (5-8) is considered a useful estimate of the magnitude of the error in the time-stretch estimate, then (5-4) becomes

$$\Delta\hat{\tau} - \Delta\tau\left(1 \pm \frac{\sqrt{6}}{\sqrt{h}\ \omega_o sT}\right) \approx \Delta\tau\left(1 \pm \frac{\sqrt{6}}{\sqrt{h}\ \omega_o T}\right)$$

so that the bias term is seen to be negligible for most situations, where $\sqrt{h}\ \omega_o T \gg \sqrt{6}$. Using the standard deviation in (5-6) yields

$$|\phi_b| - \sqrt{\frac{6}{h}} \tag{5-9}$$

This expression appears somewhat disappointing, but in practice, this large bias estimate is often due to the crudeness of the bound, rather than to poor performance of the estimator. In many situations, the time difference of arrival is known to have an upper bound (i.e., $\Delta\tau \leq \Delta\tau_{max}$), and for a given signal, one can use this "worst case" time difference in (5-5) along with the estimate of $|s-\hat{s}|$ in (5-8) to calculate an estimate of the bias, ϕ_b. Indeed, this estimator is inherently limited to estimating delays that fall within a range corresponding to the time required for the carrier to complete one cycle, i.e.

$$\phi_{min} \leq \phi \leq \phi_{min} + 2\pi$$

or

$$\omega_o s\Delta\tau_{min} \leq \omega_o s\Delta\tau \leq \omega_o s\Delta\tau_{min} + 2\pi$$

$$\Delta\tau_{min} \leq \Delta\tau \leq \Delta\tau_{max}$$

where

$$\Delta\tau_{min} = \frac{\phi_{min}}{\omega_o s} = \frac{\phi_{min}}{\omega_o}$$

$$\Delta\tau_{max} = \Delta\tau_{min} + \frac{1}{f_o}$$

In essence, a priori knowledge of the range of possible time differences is required so that one can assign the proper time-delay value to an observed phase difference. If, for example, $\Delta\tau$ is known to be small and positive then $\Delta\tau_{min}$ will be selected as zero, $\Delta\tau_{max} = \frac{1}{f_o}$ and the phase, ϕ, is defined on $(0,2\pi)$.

If, for $\Delta\tau = \Delta\tau_{max}$ the coefficients f_{1i} and f_{2i} are nearly the same then the imaginary part of the product of the two sums on the left-hand side of (5-5) will be nearly zero. For example, if the carrier frequency is 30kHz, the modulation is a 850Hz pure tone, the signal duration is 600 msec, the sampling frequency is 1700Hz, and $\tau_{min} = 0$, $\Delta\tau_{max} = \frac{1}{f_o}$, then the bias in phase is calculated numerically for real envelope signals to yield the following table:

TABLE 5-1

Phase Bias for Real Envelope Signal

Input SNR	$\Delta\tau_{max}$ (μsec)	$\lvert\phi_b\rvert$ (degrees)
20 dB	0.0333	~ 0
	0.333	9.49×10^{-6}
	3.33	1.49×10^{-4}
	33.3 ($= 1/f_o$)	1.44×10^{-3}
10 dB	0.0333	3.43×10^{-5}
	0.333	1.55×10^{-4}
	3.33	1.47×10^{-3}
	33.3	1.47×10^{-2}
0 dB	0.0333	1.97×10^{-4}
	0.333	1.54×10^{-2}
	3.33	1.63×10^{-2}
	33.3	1.65×10^{-1}

One would expect that for more complicated real-envelope waveforms with modulation frequencies no greater than 850Hz the bias values would be somewhat less than those of Table 5-1, since for lower modulation frequencies the coefficients f_{1i} and f_{2i} would be more nearly the same. Hence, the simplified numerical computations yielding Table 5-1 would provide a means of estimating the bias error of receivers utilizing more complicated real-envelope waveforms of a given bandwidth.

Because the method used to generate Table 5-1 appears to be of a more general usefulness, the process is parameterized, and the FORTRAN source code is included in Appendix C. The parameterization is useful because with it one can perform the computations once for a whole class of signals, rather than having to repeat the computations for each specific signal used. This parameterization is explained in the comments of the FORTRAN source code.

If the signal used is not a real-envelope signal as was assumed above then the above procedure is not valid, but the bias can still be evaluated numerically in the same fashion for each specific signal using the maximum time difference and the standard deviation obtained from the Cramer-Rao bound. It is mentioned here that if the signal does not have a real envelope, then in general the estimates of τ and s will in general be coupled. In this case the bound given by (5-7) will still be valid, but will not be as tight as possible. A tighter bound that accounts for τ-s coupling is discussed in Van Trees and in Cook and Bernfeld.

It is desired to combine the results of this chapter with those of previous chapters in order to come up with a rule of thumb measure of the total performance of the estimator. Here the noise will be assumed

uncorrelated (as in Chapter 3). The measure of performance to be derived will be $E\{(\phi-\phi_o)^2\}$, which represents the expectation of the squared deviations of the estimator from the true value, ϕ_o. The previous discussion in this chapter implies that the effect of the τ-s mismatch can be taken into account by replacing ϕ_o with $\phi_o + \phi_b$, where ϕ_b is a zero-mean random process with variance determined from the Cramer-Rao bound as discussed above. Without loss of generality, ϕ_o will be assumed zero, so that the variance of Figure 3-3 will now represent $E\{(\phi-\phi_b)^2\}$. The densities of Figures 3-1 and 3-2 will here be represented as $f(\phi|\phi_b)$ in accordance with the discussion following Equation 3-10. Denoting the marginal densities for the bias, ϕ_b and for the total estimate, ϕ, as $f(\phi_o)$ and $f(\phi)$, respectively, the density $f(\phi)$ can be expressed as[9]

$$f(\phi) = \int_{-\pi}^{\pi} f(\phi|\phi_b) f(\phi_b) d\phi_b .$$

Then

$$E\{(\phi-\phi_o)^2\} = E\{\phi^2\} = \int_{-\pi}^{\pi} \phi^2 \, f(\phi) d\phi$$

$$= \int_{-\pi}^{\pi} \{ \int_{-\pi}^{\pi} \phi^2 \, f(\phi|\phi_b) d\phi \} f(\phi_b) \, d\phi_b$$

where the order of integration has been interchanged. Noting that $\phi^2 = (\phi-\phi_b)^2 - \phi_b^2 + 2\phi\phi_b$, the inner integral becomes

$$\int_{-\pi}^{\pi} \phi^2 \, f(\phi|\phi_b)d\phi = \int_{-\pi}^{\pi} (\phi-\phi_b)^2 f(\phi|\phi_b)d\phi$$

$$- \phi_b^2 \int_{-\pi}^{\pi} f(\phi|\phi_b)d\phi + 2\phi_b \int_{-\pi}^{\pi} \phi f(\phi|\phi_b)d\phi \quad .$$

In this equation, it is noted that the first integral is precisely the variance σ^2, plotted in Figure 3-3, the second integral is equal to unity, and the third integral is precisely ϕ_b, so that

$$E\{(\phi-\phi_o)^2\} = \int_{-\pi}^{\pi} [\sigma^2 + \phi_b^2] f(\phi_b)d\phi_b$$

$$= \sigma^2 + \sigma_b{}^2 \, . \qquad (5\text{-}10)$$

Hence, under the assumptions stated, one may merely add the variance σ_b^2 obtained from the Cramér-Rao bound to the variance σ^2 from Figure 3-3 to obtain a rule-of-thumb value for the deviations of the estimator about the true value. Note that while this rule-of-thumb was derived for the uncorrelated noise case, it is also valid for the correlated noise case if the signal-to-noise ratio is high enough that the mean of the estimator is nearly equal to the true value, ϕ_o.

This concludes the discussion of the effects on the estimator of a τ-s mismatch. To summarize, if the time difference of arrival is small, then the only effect of a τ-s mismatch is a slight bias as in (5-4) and a decrease in the effective signal-to-noise ratio. If the time difference of arrival is not small, then the phase becomes biased. A crude estimate of this bias is given in (5-9). This estimate is independent of the properties of the signal. A better estimate can be obtained by assuming a maximum time difference, and by considering the properties of the signal employed. For real envelope signals, this process can be parameterized and computed via the program in Appendix C. For more general signals, one must use the specific signal to calculate the phase of (5-5). A mismatch in τ still affects only the effective sigal-to-noise ratio.

The variance, σ_b^2, can be added to the variances given in the graphs in the previous chapters to provide a rule-of-thumb measure of the estimator performance.

CHAPTER 6

SUMMARY AND CONCLUSIONS

It has been shown in the previous chapters that wideband signals may be used for phase-comparison time delay estimation provided the signals employed have a symmetric power spectrum. Chapter 3 analyzed the performance of the estimator operating in uncorrelated noise, while Chapter 4 discussed the performance in correlated noise. The uncorrelated assumption is often used in practice, where correlation properties of the noise may not be available.

It was shown that in correlated noise the estimator becomes biased, but approaches an unbiased estimator for favorable signal-to-noise ratios. For signal-to-noise ratios in which the densities derived are valid, the variances fall off as $\frac{1}{Nh}$, and the sample means and variances approach the derived theoretical values. By expressing the number of input samples, N, as the time-bandwidth product of the signal, the estimator was shown to use the processing gain of large time-bandwidth product signals to reduce the estimator variance.

In Chapter 5, the effects of a τ-s mismatch were examined. Central to this is the Cramér-Rao lower bound on the time-stretch estimate. A rule-of-thumb was given for estimating the squared deviations of the estimator from the true value.

This method of time delay estimation has advantages over existing methods in that it can handle Doppler shifted channels with ease, and that it can identify and estimate the time delay for resolvable scatterers each with distinct τ-s values.

Further work remains in evaluating the estimator for multiple point channels, and investigating possible interference phenomena between the different point reflectors. Also, work remains in designing signals with desirable characteristics under the new constraint that the signal's spectrum be symmetric.

Appendix A - Correlated Noise Model

This discussion of the noise correlation coefficients is taken directly from Merchant[6]. The noise model assumed here consists of two components: an incoherent component plus a coherent component, i.e.,

$$n_{ki} = n_{ki}^{i} + n_{ki}^{c} \qquad k = 1,2 \qquad \text{(B-1)}$$

where the superscript "i" denotes the incoherent component, and the superscript "c" denotes the coherent component of the noise. The variances of the real and imaginary parts of the incoherent and coherent components are σ_i^2 and σ_c^2, respectively, where

$$\sigma_n^2 = \sigma_i^2 + \sigma_c^2.$$

The incoherent noise component has the following covariance properties

$$E\{x_{1i}^{i}\, x_{2j}^{i}\} = E\{y_{1i}^{i}\, y_{2j}^{i}\} = \rho_i\, \sigma_i^2\, \delta_{ij}$$

$$E\{x_{1i}^{i}\, y_{2j}^{i}\} = E\{x_{2i}^{i}\, y_{1j}^{i}\} = 0.$$

where ρ_i is the in-phase correlation coefficient of the incoherent noise.

The coherent noise is assumed to be the same in each channel except for a phase factor:

$$n_{2i}^{c} = n_{1i}^{c}\, e^{-j\phi_c}.$$

If the ratio of the coherent noise power to the total noise power is

$$r = \frac{\sigma_c^2}{\sigma_n^2}$$

then the covariance matrix for the Gaussian density $f(x_1,y_1,x_2,y_2)$ becomes

$$R_{n_1,n_2} = \begin{bmatrix} \sigma_n^2 & 0 & \rho_i\sigma_i^2+\sigma_c^2\cos\phi_c & \sigma_c^2\sin\phi_c \\ 0 & \sigma_n^2 & -\sigma_c^2\sin\phi_c & \rho_i\sigma_i^2+\sigma_c^2\cos\phi_c \\ \rho_i\sigma_i^2+\sigma_c^2\cos\phi_c & -\sigma_c^2\sin\phi_c & \sigma_n^2 & 0 \\ \sigma_c^2\sin\phi_c & \rho_i\sigma_i^2+\sigma_c^2\cos\phi_c & 0 & \sigma_n^2 \end{bmatrix}$$

so that the noise correlation coefficients used in Chapter 4 become

$$\rho = \frac{E\{x_1x_2\}}{\sigma_n^2} = r\cos\phi_c + (1-r)\rho_i$$

$$\lambda = \frac{E\{x_1y_2\}}{\sigma_n^2} = r\sin\phi_c \ .$$

If the incoherent noise is uncorrelated between channels (i.e., $\rho_i = 0$), ρ and λ can be considered as the real and imaginary components of a "complex correlation coefficient," $\gamma = re^{-j\phi_c}$.

APPENDIX B

Change in Correlation Properties Due to Complex Multiplication

Consider two circularly symmetric complex process

$$n_1 = x_1 + jy_1$$

$$n_2 = x_2 + jy_2$$

with correlations

$$E\{x_1x_2\} = E\{y_1y_2\} = \rho\sigma^2$$

$$E\{x_1y_2\} = -E\{x_2y_1\} = \lambda\sigma^2 .$$

If these processes are each multiplied by complex numbers of unit norm, it is desired to find the new correlation properties. Let

$$u_1 + jv_1 = (a + jb)(x_1 + jy_1) = ax_1 - by_1 + j(bx_1 + ay_1)$$

$$u_2 + jv_2 = (c + jd)(x_2 + jy_2) = cx_2 - dy_2 + j(dx_2 + cy_2)$$

where (a + jb) and (c + jd) represent arbitrary complex numbers of unit norm. Then

$$\begin{aligned} E\{u_1u_2\} &= E\{(ax_1 - by_1)(cx_2 - dy_2)\} \\ &= E\{acx_1x_2 + bdy_1y_2 - adx_1y_2 - bcy_1x_2\} \\ &= [(ac + bd)\rho + (bc - ad)\lambda]\sigma^2 . \end{aligned}$$

Similarly,

$$E\{v_1 v_2\} = [(ac + bd)\rho + (bc - ad)\lambda]\sigma^2$$

$$E\{u_1 v_2\} = [(ad - bc)\rho + (ac + bd)\lambda]\sigma^2$$

$$E\{v_1 u_2\} = -[(ad - bc)\rho + (ac + bd)\lambda]\sigma^2$$

$$E\{u_1 v_1\} = E\{u_2 v_2\} = 0 \quad .$$

Two special cases are worthy of consideration. First, if both processes n_1 and n_2 are multiplied by the same number, then $a = c$ and $b = d$, so that

$$E\{u_1 u_2\} = E\{v_1 v_2\} = (a^2 + b^2)\rho\sigma^2 = \rho\sigma^2$$

$$E\{u_1 v_2\} = -E\{v_1 u_2\} = (a^2 + b^2)\lambda\sigma^2 = \lambda\sigma^2$$

where $a^2 + b^2 = c^2 + d^2 = 1$ via the assumption of unit norm multipliers. Hence if each process is multiplied by the same complex number, the correlation properties do not change.

Another special case is that in which only one channel is multiplied by a complex number, e.g., $a + jb = 1$ ($a = 1$, $b = 0$). In this case

$$E\{u_1 u_2\} = E\{v_1 v_2\} = (c\rho - d\lambda)\sigma^2$$

$$E\{u_1 v_2\} = E\{v_1 u_2\} = (d\rho + c\lambda)\sigma^2 \quad .$$

It is noted that the general case can always be broken down into consecutive application of the two special cases (i.e., let $c + jd = (a + jb)(e + jf)$).

APPENDIX C

Fortran Source Code for Phase Bias of Real-Envelope Signals

```
*  This program calculates the phase bias for real envelope
*  signals as per pp. 54-55 of this thesis (Hatlestad, J.D.,
*  "Phase Comparison Time Delay Estimation Using Wideband
*  Signals" The Pennsylvania State University, December,
*  1985).
*
*  The input parameters are as follows:
*
*  "time bandwidth product" (FBTEND) -- This parameter is
*       the time bandwidth product of the signal.  Since
*       the signal is assumed to have a real envelope the
*       bandwidth used to calculate this must be equal to
*       TWICE the maximum modulation frequency.
*
*  "ratio of bandwidth to carrier frequency" (BWRAT) -- See
*       above note for "time bandwidth product."
*
*  "ratio of time difference to modulation period"
*       (FBDELT) -- This parameter is the ratio of the
*       maximum time difference to be estimated to the
*       modulation period of the signal (1/fmax).
*       See page 55 of thesis.
*
*  "ratio of sampling frequency to bandwidth" (FSRAT) --
*        Must be greater than or equal to one.
*
*   "input signal to noise ratio" (SNR) -- Signal to noise
*        ratio in dB.
*
*****************************************************************

      COMPLEX SUMI,SUMJ,DSUM
      PI = 4.0*ATAN(1.0)
C
C  Query user for signal parameters
      WRITE(6,10)
10    FORMAT($,' Enter time-bandwidth product of signal:  ')
      READ(5,15) FBTEND
15    FORMAT(F20.10)
      FBTEND = FBTEND/2.0
      WRITE(6,20)
20    FORMAT($,' Enter ratio of bandwidth to carrier
     & frequency:  ')
      READ(5,15) BWRAT
      BWRAT = BWRAT/2.0
      WRITE(6,30)
30    FORMAT($,' Enter ratio of time difference to modulation
     & period  ')
      READ(5,15) FBDELT
```

```
      WRITE(6,40)
40    FORMAT($,' Enter ratio of sampling frequency to
     & bandwidth:  ')
      READ(5,15) FSRAT
      WRITE(6,50)
50    FORMAT($,' Enter input signal-to-noise ratio (dB):  ')
      READ(5,15) SNR
C
C  Convert SNR from dB to decimal
      SNR = 10.0**( SNR/10.0 )
C
C  Compute auxiliary variables (in radians)
      NP = NINT( FBTEND*2.0*FSRAT )
      FOTEND = FBTEND/BWRAT          ! Product of carrier and
C                                        signal duration
      FBTINCR = FBTEND/FLOAT(NP)     ! Product of bandwidth and
C                                        time increment
      FOTINCR = FOTEND/FLOAT(NP)     ! Product of carrier and
C                                        ti-e increment
C
      DELS = SQRT(6.0/SNR)/(2.0*PI*FOTEND) ! Expected error
C                                            for s estimate
      S = 1.0 + DELS
C
C  Convert arguments of trigonometric functions to radians
      FBTINCR = 2.0*PI*FBTINCR
      FOTINCR = 2.0*PI*FOTINCR
      FBDELT = 2.0*PI*FBDELT
C
C  Intialize sums
      SUMI = CMPLX(0.0,0.0)
      SUMJ = CMPLX(0.0,0.0)
C
C  Compute first sum
      DO I=0,NP
       COSCOSI=COS( I*FBTINCR )*COS( S*I*FBTINCR )
       SUMI=SUMI + COSCOSI*CEXP( CMPLX(0.0,DELS*I*FOTINCR) )
      ENDDO
C
C  Compute second sum
      DO J=0,NP
       COSCOSJ=COS( J*FBTINCR )*COS( S*(J*FBTINCR+FBDELT) )
       SUMJ=SUMJ+COSCOSJ*CEXP( CMPLX(0.0,-DELS*J*FOTINCR) )
      ENDDO
C
C  Multiply sums
      DSUM = SUMI*SUMJ
C
C  Compute phase bias
      PHIB = ATAN( AIMAG(DSUM)/REAL(DSUM) )
      PHIB = PHIB*180.0/PI
      WRITE(6,60) PHIB
60    FORMAT(' PHIB (DEGREES)  =  ',E10.4)
C
STOP
END
```

BIBLIOGRAPHY

1. IEEE Transactions on Acoustic, Speech and Signal Processing Vol. ASSP-29, No. 3, Part II: Special Issue on Time Delay Estimation, 1981.

2. Rainal, A. J., "Monopulse Radars Excited by Gaussian Signals," IEEE Transactions on Aerospace and Electronic Systems Vol. AES-2, No. 3, pp. 337-345, May 1966.

3. Knapp, C. H., Carter, G. C., "The Generalized Correlation Method for Estimation of Time Delay," IEEE Transactions on Acoustics, Speech and Signal Processing Vol. ASSP-24, No. 4, pp. 320-327, August, 1976

4. Hamon, B. V., Hannon, E. J., "Spectral Estimation of Time Dealy for Disersive and Non-Dispersive Systems," Applied Statistics, Vol. 23, No. 2 pp. 134-142, 1974.

5. Fenlon, F. H., Private Communications.

6. Merchant, C. C., Detection of a Dual Channel Differential Phase Modulated Signal in Correlated Noise, Masters Thesis, The Pennsylvania State University, 1982.

7. Ricker, D. W., "Small Aperture Angle Measurement for Active Echo Location Systems," IEEE Transactions on Aerospace and Electronic Systems, (Under review).

8. Papoulis, A., Probability, Random variables and Stochastic Processes, pp. 133-134, New York: McGraw-Hill, 1984.

9. Larson, H. J., Shubert, B. O., Probabilistic Models in Engineering Sciences, Volume I, pp. 192-196, New York: John Wiley and Sons, 1979.

10. Van Trees, H. L., Detection, Estimation and Modulation Theory, Part III, New York: John Wiley and Sons, 1971.

11. Cook, C. E., Bernfeld, M., Radar Signals, New York: Academic Press, 1967.

12. Altes, R. A., "Some Invariance Properties of the Wide Band Ambiguity Function," Journal of the Acoustical Society of America, Vol. 53, No. 4, pp. 1154-1160, 1973.

13. Altes, R. A., "Target Position Estimation in Radar and Sonar, and Generalized Ambiguity Analysis for Maximum Likelihood Parameter Estimation," Proceedings of the IEEE, Vol. 67, No. 6, June 1979.

14. Sorenson, H. W., Parameter Estimation, Principles and Problems, pp. 183-184, New York: M. Dekker, 1980.

BIBLIOGRAPHY (Continued)

15. Whalen, A. D., Detection of Signals in Noise, pp. 324-325, New York: Academic Press, 1971.

16. Gradshteyn, I. S., Ryzhik, I.M., Table of Integrals, Series and Products, p. 338, New York: Academic Press, 1980.

17. Golomb, S. W., Algebraic Constructions for Costes Arrays, Journal of Combinational Theory, Series A 37, pp. 13-21, 1984.

18. Rife, D. C., Vincent, G. A., "Use of the Discrete Fourier Transform in the Measurement of Frequencies and Levels of Tones," Bell Systems Technical Journal, Vol. 49, No. 2, pp. 197-228, February 1970.

19. Strang, G., Linear Algebra and Its Applications, p. 250, New York: Academic Press, 1980.

DISTRIBUTION LIST FOR ARL TM 85-136, by J. A. Hatlestad, dated 31 July 1985

Commander
Naval Sea Systems Command
Department of the Navy
Washington, DC 20362

Attn: Dr. P. H. Kurtz, PMS 406B
Copy No. 1

Attn: Mr. D. Porter, PMS 407
Copy No. 2

Attn: Mr. F. J. Romano, SEA 63R-3
Copy No. 3

Attn: Code SEA 9961 (Library)
Copies 4 and 5

Commander
Office of Naval Technology
Department of the Navy
800 N. Quincy Street
Arlington, VA 22217

Attn: Mr. D. C. Houser, SEA 63R-34
Copy No. 6

Attn: Dr. A. J. Faulstich, Mat 0716
Copy No. 7

University of Washington
Applied Physics Laboratory
1013 N. E. 40th Street
Seattle, WA 98105

Attn: Mr. C. Eggen
Copy No. 8

Naval Underwater Systems Center
Department of the Navy
Newport, RI 02840

Attn: Dr. J. R. Short, Code 303
Copy No. 9

END

FILMED

5-86

DTIC